Preclinical Characterization of (*R*)-3-((3*S*,4*S*)-3-fluoro-4-(4-hydroxyphenyl)piperidin-1-yl)-1-(4-methylbenzyl)pyrrolidin-2-one (BMS-986169), a Novel, Intravenous, Glutamate N-Methyl-D-Aspartate 2B (GluN2B) Receptor Negative Allosteric Modulator with Potential in Major Depressive Disorder

Linda J Bristow, Jyoti Gulia, Michael R Weed, Bettadapura N Srikumar, Yu-Wen Li, John D Graef, Pattipati S Naidu, Charulatha Sanmathi, Jayant Aher, Tanmaya Bastia, Mahesh Paschapur, Narasimharaju Kalidindi, Kuchibhotla Vijaya Kumar, Thaddeus Molski, Rick Pieschl, Alda Fernandes, Jeffrey M Brown, Digavalli V Sivarao, Kimberly Newberry, Mark Bookbinder, Joseph Polino, Deborah Keavy, Amy Newton, Eric Shields, Jean Simmermacher, James Kempson, Jianqing Li, Huiping Zhang, Arvind Mathur, Raja Reddy Kallem, Meenakshee Sinha, Manjunath Ramarao, Reeba K Vikramadithyan, Srinivasan Thangathirupathy, Jayakumar Warrier, Joanne J Bronson, Richard E Olson, John E Macor, Charlie F Albright, Dalton King, Lorin A Thompson, Lawrence R Marcin, Michael Sinz.

Neuroscience Discovery Biology (L.J.B., M.R.W., Y.-W.L., J.D.G., T.M., R.P., A.F., J.M.B., D.V.S., K.N., M.B., J.P., D.K., A.N., C.F.A.), Neuroscience Discovery Chemistry (J.J.B, R.E.O., J.E.M., D.K., L.A.T., L.R.M.), Preclinical Candidate Optimization (E.S., J.S., M.S.), Bristol-Myers Squibb Company, Wallingford, Connecticut, USA; Discovery Synthesis, Bristol-Myers Squibb Company, Lawrenceville, Princeton, NJ, USA (J.K., J.L., H.Z., A.M.); Biocon Bristol-Myers Squibb Research Center, Bangalore, India (J.G., B.N.S., P.S.N., C.S., J.A., T.B., M.P., N.K., K.V.K., R.R.K., M.S., M.R., R.K.V., S.T., J.W.).

JPET Fast Forward. Published on September 27, 2017 as DOI: 10.1124/jpet.117.242784
This article has not been copyedited and formatted. The final version may differ from this version.

JPET #242784

Running Title: Preclinical characterization of the GluN2B NAM BMS-986169

Corresponding authors

Linda J Bristow; Bristol-Myers Squibb Company, 5 Research Parkway, Wallingford, CT 06492. Tel: 203-677-6701; Fax: 203-677-7702; e mail: brislj100@gmail.com

Lawrence Marcin; Bristol-Myers Squibb Company, 5 Research Parkway, Wallingford, CT 06492. Tel: 203-677-6701; Fax: 203-677-7702; email: lawrence.marcin@bms.com

Number of Text pages: 62

Number of Tables: 1

Number of Figures: 10

Number of References: 51

Number of words - Abstract: 244 words

Number of words - Introduction: 749 words

Number of words - Discussion: 1498 words

Nonstandard abbreviations: aCSF, artificial cerebrospinal fluid; AKT, protein kinase B; AMPA, α-amino-3-hydroxy-5-methyl-4-isoxazolepropionic acid receptor; ANOVA, analysis of variance; ATD, amino terminal domain; AUC, area under the curve; BBRC, Biocon Bristol-Myers Squibb Research Center; BDNF, brain derived neurotrophic factor; BMS, Bristol-Myers Squibb; CANTAB, Cambridge Neuropsychological Test Automated Battery; CP-101,606, (1*S*,2*S*)-1-(4-hydroxyphenyl)-2-(4-hydroxy-4-phenylpiperidino)-1-

propanol; CSF, cerebrospinal fluid; DMS, delayed match to sample; eEF2, eukaryotic elongation factor 2; ERK, extracellular signal-regulated kinase; fEPSP, field excitatory postsynaptic potential; FST, forced swim test; GluN1a, glutamate N-methyl-D-aspartate receptor 1a subunit; GluN2A, glutamate N-methyl-D-aspartate receptor 2A subunit; GluN2B, glutamate N-methyl-D-aspartate receptor 2B subunit; GluN2C, glutamate N-methyl-D-aspartate receptor 2C subunit; GluN2D, glutamate N-methyl-D-aspartate receptor 2D subunit; GluR1, glutamate ionotropic receptor AMPA subtype subunit 1; HFS, high frequency stimulation; hERG, human Ether-a-go-go-related gene potassium channel; i.p., intraperitoneal; i.v., intravenous; LC-MS/MS, liquid chromatography-mass spectrometry/mass spectrometry; LMA, locomotor activity; LTP, long term potentiation; MDD, major depressive disorder; MK-0657 (CERC-301), 4-Methylbenzyl-(3*S*,4*R*)-3-fluoro-4-[(2-pyrimidinylamino)methyl]-1-piperidinecarboxylate; mTOR, mechanistic target of rapamycin; mTORC1, mechanistic target of rapamycin complex 1; NAM, negative allosteric modulator; NBQX, 2,3,dihydroxy-6-nitro-7-sulfamoyl-benzo[f]quinoxaline-2,3-dione; NSF, novelty suppressed feeding; NMDA, N-methyl-D-aspartate; PEI, polyethylenimine; PSD95, postsynaptic density 95; qEEG, quantitative electroencephalogram; RM, repeated measures; Ro 25-6981, 4-[(1R,2S)-3-(4-benzylpiperidin-1-yl)-1-hydroxy-2-methylpropyl]phenol; SSRI, selective serotonin reuptake inhibitor; TRD, treatment resistant depression.

Recommended section assignment: Neuropharmacology

Abstract

(R)-3-((3S,4S)-3-fluoro-4-(4-hydroxyphenyl)piperidin-1-yl)-1-(4-methylbenzyl)pyrrolidin-2-one (BMS-986169), and the phosphate prodrug (BMS-986163), were identified from a drug discovery effort focused on the development of novel, intravenous, glutamate N-methyl-D-aspartate 2B receptor (GluN2B) negative allosteric modulators for treatment resistant depression (TRD). BMS-986169 showed high binding affinity for the GluN2B subunit allosteric modulatory site (Ki = 4.03-6.3 nM) and selectively inhibited GluN2B receptor function in Xenopus oocytes expressing human N-methyl-D-aspartate receptor subtypes (IC50 = 24.1 nM). BMS-986169 weakly inhibited human Ether-a-go-go-related gene (hERG) channel activity (IC50 = 28.4 micromolar) and had negligible activity in an assay panel containing 40 additional pharmacological targets. Intravenous administration of BMS-986169 or BMS-986163, dose-dependently increased GluN2B receptor occupancy and inhibited in vivo [3H]MK-801 binding confirming target engagement and effective cleavage of the prodrug. BMS-986169 reduced immobility in the mouse forced swim test, an effect similar to intravenous ketamine treatment. Decreased novelty suppressed feeding latency and increased ex vivo hippocampal long term potentiation was also seen 24 hours after acute BMS-986163 or BMS-986169 administration. BMS-986169 did not produce ketamine-like hyperlocomotion or abnormal behaviors in mice or cynomolgus monkeys but did produce a transient working memory impairment in monkeys that was closely related to plasma exposure. Finally, BMS-986163 produced robust changes in the quantitative electroencephalogram power band distribution, a translational measure that can be used to assess pharmacodynamic activity in healthy humans. Due to the poor aqueous

solubility of BMS-986169, BMS-986163 was selected as the lead GluN2B NAM candidate for further evaluation as a novel intravenous agent for TRD.

Introduction

Major depressive disorder (MDD) is a prevalent disease and a leading cause of global disability (Ustün et al., 2004). In the USA alone, recent reports show a prevalence of 6.8% with 15.4 million individuals affected and an overall economic burden of ~$200 billion (Greenberg et al., 2015). While therapeutics targeting the monoaminergic systems have been available for many years, many patients fail to show an adequate treatment response. In this regard, results from the STAR*D (Sequenced Treatment Alternatives to Relieve Depression) study showed that only 1/3rd of patients treated with a selective serotonin reuptake inhibitor (SSRI) achieved remission, with 40% of those requiring more than 8 weeks of treatment for resolution of their symptoms (reviewed in Gaynes et al., 2009). An additional 50% of patients showed partial improvement but still exhibited residual symptoms (McClintock et al., 2011) which increases the probability of future relapse and poorer functional and psychosocial outcomes (Paykel et al., 1995; Fava 2006). Finally, almost 1/3rd of patients were resistant to treatment and failed to respond to additional antidepressant drug switching and augmentation approaches. Clearly a high unmet medical need exists for new agents with novel mechanisms that show rapid and improved efficacy in patients with MDD and treatment resistant depression (TRD).

In the search for novel mechanisms, N-methyl-D-aspartate (NMDA) receptor antagonists have received intense investigation following the first demonstration that the non-selective NMDA receptor channel blocker, ketamine, is efficacious in TRD patients

JPET Fast Forward. Published on September 27, 2017 as DOI: 10.1124/jpet.117.242784
This article has not been copyedited and formatted. The final version may differ from this version.

(Berman et al., 2000). The clinical response to ketamine was remarkable in that a single, intravenous (i.v.), sub-anesthetic dose produced rapid symptom relief within hours of dosing that was sustained for up to 7 days. Subsequent studies have confirmed that acute ketamine treatment rapidly achieves a 66-77% response rate and 31% remission rate in TRD patients and have also extended these findings to patients with bipolar depression (reviewed in Lener et al., 2017). While this unique efficacy profile is widely accepted, ketamine also produces undesirable effects including transient dissociative and psychotomimetic effects that emerge during the infusion but resolve within ~2 hours of dosing and may therefore be manageable within the treatment environment. However, additional concerns including the potential for neuronal injury and abuse have led to the search for alternative approaches that may retain the efficacy profile of ketamine but with fewer liabilities. In this regard, agents that selectively inhibit the glutamate NMDA 2B (GluN2B) receptor subtype have received attention. This target has been the focus of extensive drug development efforts aimed at the treatment of conditions such as stroke, Parkinson's disease and chronic pain (Layton et al., 2006). GluN2B receptors possess an amino terminal domain (ATD) allosteric binding site that can be targeted to develop subtype selective, negative allosteric modulators (NAMs) (Mony et al., 2009). In a small proof of concept study in SSRI resistant MDD patients, a single i.v. administration of the GluN2B NAM, CP-101,606, achieved a 60% response rate and 30% remission rate 5 days after dosing with an infusion regimen that produced minimal dissociative effects (Preskorn et al., 2008).

Preclinical results also show that GluN2B NAMs have a ketamine-like antidepressant profile and that the effects of ketamine may involve the GluN2B receptor subtype. Acute treatment with the GluN2B NAM, Ro 25-6981 activates the mTOR signaling pathway and increases synaptic protein expression, effects thought to underlie the rapid antidepressant effect of ketamine (Li et al., 2010). Direct infusion of the mTOR inhibitor rapamycin into the medial prefrontal cortex prevents the antidepressant-like behavioral effects of Ro 25-6981 and treatment with the AMPA receptor antagonist, NBQX, inhibits antidepressant activity and mTOR pathway activation after acute ketamine or Ro 25-6981 administration suggesting common mechanisms (Li et al., 2010; Maeng et al., 2008). On the other hand, genetic deletion of GluN2B subunits in cortical pyramidal neurons mimics and occludes the effects of ketamine on mTOR pathway activation and synaptic protein synthesis, excitatory synaptic transmission and depression-like behavior (Miller et al., 2014). While it should be acknowledged that not all groups are able to demonstrate the mTOR pathway activation effect of ketamine (Popp et al., 2016), these results have led to renewed interest in GluN2B NAMs and their potential as rapid acting antidepressant agents for TRD (Miller et al., 2016).

The present studies describe the pharmacological characterization of BMS-986169 ((*R*)-3-((3*S*,4*S*)-3-fluoro-4-(4-hydroxyphenyl)piperidin-1-yl)-1-(4-methylbenzyl)pyrrolidin-2-one), a novel GluN2B NAM identified during a drug discovery program focused on the identification of an i.v. therapeutic for TRD. We also present results for BMS-986163, the phosphate prodrug of BMS-986169, which was developed to address the poor aqueous solubility of the parent molecule.

Materials and Methods

Animals

Studies were conducted at either Bristol-Myers Squibb (BMS, Wallingford CT, USA) or at the Biocon Bristol-Myers Squibb Research Center (BBRC, Bangalore, India).

BMS Studies

Animals were housed in an Association for Assessment and Accreditation of Laboratory Animal Care accredited facility and maintained in accordance with the guidelines of the Animal Care and Use Committee of the Bristol-Myers Squibb Company, the “Guide for Care and Use of Laboratory Animals” and the guidelines published in the National Institutes of Health Guide for the Care and Use of Laboratory Animals. Research protocols were approved by the Bristol-Myers Squibb Company Animal Care and Use Committee. In vivo [^{3}H]MK-801 binding studies were conducted in singly housed, male Sprague Dawley rats (170-250 g; ~6-8 weeks of age) supplied with a previously implanted jugular vein catheter (Hilltop Lab Animals Inc., Scottsdale, PA). Ex vivo GluN2B occupancy studies were conducted in male Sprague Dawley rats housed 2 rats/cage purchased from Charles River Laboratories (Raleigh, NC; 5-7 weeks of age) or Harlan (Indianapolis, IN; 7-9 weeks of age). Ex vivo LTP studies were conducted in male Sprague Dawley rats housed 2 rats/cage purchased from Harlan (Indianapolis, IN; 4-6 weeks of age). Cage size for both single and pair housed rats was 10.25 x 14 inches and animals were housed in temperature (21 ± 2°C) and humidity (50 ± 10%) controlled rooms maintained under a 12 h light/dark cycle (lights on at 06.00 h) with food and water available *ad libitum*. Cognitive performance, behavioral observational

studies and qEEG studies were conducted in separate cohorts of male cynomolgus monkeys (Macaca Fasicularis; 5-7 years of age; 5.0-8.5 kg). Monkeys were typically pair housed (cage size (width/depth/height): 64 x 31 x 33 inches) and fed standard monkey chow (Harlan Teklad global 20% protein Primate Diet 2050); subjects for cognitive testing were fed sufficient quantities to ensure normal growth while maintaining motivation to perform cognitive tasks (Weed et al., 1999); subjects for behavioral observation were food restricted overnight prior to compound administration. For all subjects, water was continuously available except during studies and fresh fruit or dietary enrichment was provided twice weekly. Toys and foraging devices were routinely provided and television programs were available in the colony rooms. Subjects were fitted with plastic or metal neck collars (Primate Products, Immokalee, FL).

BBRC Studies

All experimental procedures were conducted in accordance with the guidelines set by the Committee for the Purpose of Control and Supervision on Experiments on Animals (CPCSEA), Ministry of Environment and Forests, Government of India. An Institutional animal ethics committee approved the experimental protocols and all animals were housed in an Association for Assessment and Accreditation of Laboratory Animal Care accredited animal facility. Female Xenopus laevis were obtained from Nasco (Fort Atkinson, WI) and housed 2 frogs/cage in Tecniplast XenopLus standalone housing. Water temperature and pH were maintained at 18 ± 1°C and 6.8-7.4 respectively with regular monitoring of nitrogenous wastes. Frogs were fed with Zeigler adult Xenopus diet (Xenopus Express, Brooksville, FL) 3 times/week and each cage was provided with enrichment tubes and pads. Male Sprague Dawley rats (7-10 weeks of age; Harlan,

Netherlands) were used for *in vitro* GluN2B binding studies and were housed 3 rats/cage (cage size: 12.6 x 12 inches). Male CD-1 mice were obtained directly from Harlan (Netherlands) for GluN2B occupancy (5-8 weeks of age) and locomotor activity (LMA) studies (6-7 weeks of age) or from in house breeding colonies derived from Harlan CD-1 mice for the forced swim test (FST; 6-7 weeks of age). Novelty suppressed feeding (NSF) studies were conducted in male BALB/c mice (13-14 weeks of age, Taconic Vivo-bio, Hyderabad, India). Mice were housed 5/cage (cage size: 12.8 x 6.6 inches) and all rodents were held in colony rooms with controlled temperature (22-24°C) and humidity (48-54%) under a 12 h light-dark cycle (lights on at 07:00 h) with food and water available *ad libitum* unless specified otherwise.

Reagents

BMS-986169 ((*R*)-3-((3*S*,4*S*)-3-fluoro-4-(4-hydroxyphenyl)piperidin-1-yl)-1-(4-methylbenzyl)pyrrolidin-2-one), BMS-986163 (4-((3*S*,4*S*)-3-fluoro-1-((*R*)-1-(4-methylbenzyl)-2-oxopyrrolidin-3-yl)piperidin-4-yl)phenyl dihydrogen phosphate), CP-101,606 (Traxoprodil; free base (in vitro studies) or methane sulfonic acid salt), Ro 25-6981, MK-0657 (CERC-301), [^{3}H]Ro 25-6981 and [^{3}H]MK-801 were synthesized by the BMS or BBRC Chemistry groups or the BMS Radiosynthesis group. The chemical structure of BMS-986169 and the phosphate prodrug BMS-986163 are shown in Figure 1. Sources of other reagents were as follows: (+)MK-801 hydrogen maleate (Sigma-Aldrich, St Louis, MO), Ketamine HCl (Ketaset, Fort Dodge Animal Health, Fort Dodge, IA or Aneket, Neon Pharmaceuticals, Mumbai, India), Ro-04-5595 (Tocris Bioscience, Bristol, UK).

GluN2B Binding Ki Determinations in vitro

JPET Fast Forward. Published on September 27, 2017 as DOI: 10.1124/jpet.117.242784
This article has not been copyedited and formatted. The final version may differ from this version.

Studies to determine *in vitro* binding affinity at rat brain GluN2B receptors were conducted at BBRC. For membrane preparation, rat forebrains were thawed on ice for 20 min in homogenization buffer composed of 50 mM KH_2PO_4 (pH adjusted to 7.4 with KOH), 1 mM EDTA, 0.005% Triton X-100 and protease inhibitor cocktail (1:1000; Sigma Aldrich). Thawed brains were homogenized using a Dounce homogenizer and centrifuged at 48,000 g for 20 min. The pellet was re-suspended in cold buffer and homogenized again using a Dounce homogenizer. Finally, the protein concentration was determined using a BCA kit (Sigma Aldrich) and the homogenate was aliquoted, flash frozen and stored at -80˚C for 3-4 months. To perform competition binding experiments, thawed membrane was passed through a 24 gauge needle and 98 µl (20 µg) of the membrane protein added to each well of a 96 well plate. Test compounds (2 µl) were added to achieve the desired concentration in each well of the assay plate, incubated with brain membrane for 15 min followed by the addition of [^{3}H]Ro 25-6981 (50 µl, 4 nM final concentration) and further incubation for 1 h. Non-specific binding was determined using MK-0657 (40 µM). Membranes were then harvested onto GF/B filter plates using a Filtermate universal harvester (Perkin Elmer). Prior to membrane transfer, filter plates were presoaked in 0.5% PEI for 1 h at room temperature and washed 3 times using cold assay buffer. After membrane transfer, filter plates were washed 8 times with cold assay buffer and dried at 50˚C for 20 min followed by addition of 50 µl of Microscint20 scintillation cocktail (Perkin Elmer). Radioactivity was counted using a TopCount (Perkin Elmer) after 10 min of Microscint addition. Counts per minute were converted to % inhibition and the concentration response curves plotted and fitted

JPET Fast Forward. Published on September 27, 2017 as DOI: 10.1124/jpet.117.242784
This article has not been copyedited and formatted. The final version may differ from this version.

to calculate Ki values using custom made software. Each experiment had a plate duplicate and was repeated at least twice to obtain an average binding Ki value.

Studies to determine *in vitro* binding affinity at human (Analytical Biological Services Inc., Wilmington, DE) and cynomolgus monkey GluN2B receptors were conducted at BMS. Frontal cortical membranes were prepared from frozen brain sections by homogenizing samples at 4˚C in hypotonic lysis buffer consisting of 10 mM Tris (pH 7.4), 5 mM EDTA and protease inhibitors and centrifugation at 32,000g for 20 min. The pellet was washed once in buffer consisting of 50 mM Tris (pH 7.4), 1 mM EDTA and protease inhibitors and centrifuged at 32,000 g for 20 min. This pellet was then re-suspended in buffer containing 50 mM KH_2PO_4 (pH 7.4 at 25˚C), 1 mM EDTA, 0.005% Triton X-100 and 0.1% (v/v) Sigma Protease Inhibitor Cocktail. Aliquots were then frozen on dry ice/ethanol and kept at -80˚C. On the day of the assay, frozen aliquots of membrane homogenate were thawed, homogenized and re-suspended to provide 15 µg/well cynomolgus brain protein or 35 µg/well human brain protein in assay buffer (5 mM Tris-Cl, pH 7.4). In saturation binding experiments, the membrane preparation was incubated at room temperature for 120 min in the presence of increasing concentrations of [^{3}H]Ro 25-6981. Non-specific binding was defined with 10 µM Ro-04-5595. Competition binding experiments were performed using a single concentration of [^{3}H]Ro 25-6981 (1.5 nM) in the presence of 10 increasing concentrations (in duplicate) of test compound. The reaction was terminated by the addition of 5 ml of ice-cold assay buffer and rapid vacuum filtration through a Brandel Cell Harvester using Whatman GF/B filters presoaked in 0.5% PEI. The filtration and washing was completed in less than 30 s. The filter was then punched onto a 96 well microbeta sample plate, 200 µl/well of

Packard Ultima Gold XR scintillation fluid added and the filters soaked overnight. The filter pads were then counted in a LKB Trilux liquid scintillation counter. Ki values from inhibition curves were determined using the “sigmoidal dose-response (variable slope)” non–linear curve fit by GraphPad Prism (v5.01).

Functional Inhibition of NMDA receptor subtypes in vitro

Studies to demonstrate functional inhibition of GluN2B receptor mediated currents in Xenopus oocytes were conducted at BBRC. Prior to surgery, frogs were anesthetized using 3-amino-benzoic acid ethyl ester (1g/l, pH 7.0 adjusted using sodium bicarbonate), the ovarian lobes removed using aseptic surgical techniques, and the animals then singly housed for a 24 h recovery period with post-operative monitoring for up to a week post-surgery. Following removal the ovarian lobes were incubated in cold Xenopus oocyte buffer A (Biopredic International; Saint Gregoire, France) for 1 h. The oocytes were then mechanically isolated in small clusters followed by collagenase treatment (1.5 to 2 mg/ml) for at least 1 h on a shaking platform at 18˚C to remove the follicular layer. The defolliculated oocytes were treated with Xenopus oocyte buffer A, B and C (Biopredic International) for 15 min each in series at 18˚C and then maintained in Barth’s solution (pH 7.4) composed of 88 mM NaCl, 1 mM KCl, 2.4 mM $NaHCO_3$, 10 mM HEPES, 0.82 mM $MgSO_4$, 0.33 mM $Ca(NO_3)_2$, 0.91 mM $CaCl_2$ and supplemented with gentamycin (100 µg/ml), penicillin (10 µg/ml) and streptomycin (10 µg/ml). To determine functional inhibition of GluN2B receptors, oocytes were injected with 8-15 ng each of human GluN1a and GluN2B cRNA within 24 h of isolation. Two electrode voltage clamp recordings were made 2-7 days post injection. Oocytes were placed in a plexiglass chamber and impaled with glass microelectrodes filled with 3M KCl. The

oocytes were clamped at -40 mV and perfused with buffer containing 90 mM NaCl, 1 mM KCl, 10 mM HEPES, 0.01 mM EDTA and 0.5 mM $BaCl_2$, pH 7.4. NMDA receptor currents were activated by the application of 50 µM glutamate and 30 µM glycine and recorded using an Axoclamp 900A amplifier and pClamp 10 data acquisition software. The concentration response was determined using 4-7 concentrations of the test compound and each concentration was applied for 15-20 min on a different oocyte. The baseline leak current at -40 mV was recorded at the beginning and the end of the recording and the full current trace was linearly corrected for any change in leak current. The level of inhibition was expressed as percent of the initial glutamate/glycine response in the absence of compound and the IC_{50} values were obtained by concentration response curve fitting using the following equation in GraphPad Prism (v5.01): Y=Bottom + (Top-Bottom)/(1+10^((LogIC_{50}-X)*HillSlope)) where X= log of concentration, Y= % inhibition and the top and bottom were constrained to 100 and 0, respectively. To determine functional inhibition at other NMDA receptor subtypes, isolated oocytes were injected with 0.2-0.5 ng of human GluN1a and 0.5-1 ng of human GluN2A or 45-60 ng of human GluN1a and 35-55 ng of human GluN2C or GluN2D. The voltage clamp recording procedure was as described above except that oocytes were clamped at -80 mV to record GluN2C or GluN2D receptor currents and compound was applied at 3 µM only for 10-15 min. The level of inhibition at 3 µM was calculated as a percent of the initial glutamate/glycine mediated current.

Ex vivo GluN2B Occupancy in Mice and Rats

Studies to determine *ex vivo* GluN2B occupancy in rats were conducted at BMS. For dose response studies rats (n = 4-5/group) were randomly assigned to receive an i.v.

injection via the tail vein of either vehicle (0.9% saline, pH 7.4 for BMS-986163 or 30% hydroxypropyl-β-cyclodextrin/70% citrate buffer, pH 4 for BMS-986169; 2 ml/kg), BMS-986169 (0.03, 0.3, 1 or 3 mg/kg) or BMS-986163 (0.1, 0.3, 1, 3 or 10 mg/kg) 15 min prior to decapitation and blood and brains collected. In a separate study the time course of GluN2B occupancy was determined from 5-120 min after i.v. dosing with 3 mg/kg BMS-986169 (n = 4/group). In addition to collection of plasma and brain a terminal CSF sample was also collected from the cisterna magna for measurement of drug concentrations. Finally, in parallel with [^{3}H]MK-801 binding studies, satellite groups of rats with jugular vein catheters were randomly assigned to receive i.v. BMS-986163 or vehicle treatment (n = 3/group) to determine GluN2B occupancy and drug exposure. Following collection the brain was placed on ice, the cerebellum removed and the forebrain dissected along the midline into left and right hemispheres, snap frozen in isopentane on dry ice and stored at -80˚C. Blood samples were centrifuged at 3500 rpm for 5 min at 4˚C to separate the plasma and plasma and CSF samples were stored at -80˚C. On the day of occupancy determinations one forebrain hemisphere from each animal was thawed and homogenized in 7 volumes of an assay buffer containing 50 mM KH_2PO_4, 1 mM EDTA, 0.005% Triton-X100, 1:1000 dilution of Sigma protease inhibitor P3843 (pH 7.4) using a polytron homogenizer. In a 96-well plate, 100 µg of tissue (0.4 mg/ml; tested in triplicate) was incubated with 5 nM [^{3}H]Ro 25-6981 in the assay solution at 4°C for 5 min. The non-specific binding was defined by inclusion of 10 µM Ro 25-6981. At the end of the incubation, the reaction was stopped by filtration through FPXLR-196 filters that had been soaked in 0.5-1.0% PEI for 1 h at 4°C. The filters were washed twice with ice-cold assay solution, and the radioactivity was

measured using a Wallac Microbeta liquid scintillation counter. For each sample, specific binding was calculated by subtracting the value of the non-specific binding from that of the average total binding and % occupancy calculated as (1- specific binding in drug treated/specific binding in vehicle treated) x 100%. For estimation of the dose producing 50% GluN2B occupancy (Occ50), a one-site binding model using nonlinear regression was fitted to the mean occupancy achieved at each dose (GraphPad Prism v7.02). To estimate the Occ50 drug concentration in plasma, brain or CSF the same curve fit was applied to plots of occupancy/exposure results for individual subjects.

Additional GluN2B occupancy determinations were also conducted at BBRC in mice completing behavioral assessment in FST (n = 4/group) or in satellite groups dosed in parallel with NSF and LMA subjects (n = 4/group). Mice were rapidly decapitated and the brain and blood samples collected. Forebrain membranes were prepared as above except for addition of 3 ml assay buffer for 160 mg tissue and homogenization by Polytron for 10 s followed by 30 strokes using a Dounce homogenizer. On the day of the experiment, brain homogenates were thawed on ice and passed three times through a 24 gauge needle. In a 96 well plate 200 µl (6.4 mg/ml) tissue homogenate (tested in triplicate) was incubated with 6 nM [^{3}H]Ro 25-6981 in assay buffer at 4˚C for 5 min on a shaking platform. The membrane was harvested onto a GF/B filter plate (treated with 0.5% PEI for 1 h at 4˚C), the filter plate was then dried at 50˚C for 20 min and 50 µl of Microscint20 (Perkin Elmer) was added. After shaking the filter plate for 10 min, the radioactivity was measured using a TopCount (Perkin Elmer). Non-specific binding was determined by incubating the membrane from vehicle-treated animals with 10 µM of Ro 25-6981.

JPET Fast Forward. Published on September 27, 2017 as DOI: 10.1124/jpet.117.242784
This article has not been copyedited and formatted. The final version may differ from this version.

In vivo [^{3}H]MK-801 binding in rats

Studies to determine inhibition of *in vivo* [^{3}H]MK-801 binding were conducted at BMS using methods previously described (Fernandes et al., 2015). For the dose response study rats with previously implanted jugular vein catheters were randomly assigned (n = 4/group) to treatment with either vehicle (0.9% saline, 2 ml/kg i.v.), BMS-986163 (0.1, 0.3, 1, 3, 10 or 30 mg/kg, i.v.) or MK-801 (5 mg/kg, i.v.) to define the specific binding window. All rats received [^{3}H]MK-801 (0.2 µCi/g body weight) 5 min later and were decapitated 10 min after [^{3}H]MK-801 administration (i.e. 15 min after BMS-986163 treatment). For the time course study, rats (n = 4/group) were dosed with BMS-986163 (3 mg/kg, i.v.) 5-120 min prior to euthanasia with all subjects receiving [^{3}H]MK-801 10 min prior to sacrifice. At the appropriate time point the brain was collected, the cerebellum and brain stem removed and one forebrain hemisphere weighed and homogenized in 30 volumes of ice-cold 5 mM Tris-acetate buffer (pH 7.0). A 600 µl sample of the homogenate was filtered through GF/B Whatman filters (presoaked in ice-cold Tris-acetate buffer) on a filter box connected to a vacuum source. Filters were washed 4 times with ice-cold Tris-acetate buffer, and then placed in a scintillation vial with 10 ml of scintillation fluid (Optiphase supermix, Perkin Elmer) overnight. Radioactivity in the scintillation vial was counted using a Wallac Microbeta liquid scintillation counter. The total [^{3}H]MK-801 binding was determined by measuring radioactivity in the forebrain of animals treated with vehicle whereas non-specific binding was determined by measuring the radioactivity in animals treated with MK-801. For each sample, specific binding was calculated by subtracting the value of the non-specific binding from that of the total binding and % inhibition calculated as (1- specific

binding in drug treated/specific binding in vehicle treated) x 100%. For estimation of the dose producing 50% inhibition of MK-801 binding, data were fitted to a one-site binding model using nonlinear regression as described previously.

Mouse Forced Swim Test (FST)

Studies to evaluate GluN2B NAM treatment effects on immobility in the mouse FST were conducted at BBRC. All studies were conducted between 09.00-13.30 h and were performed under dim light and low noise conditions. Behavior was recorded and quantified using the automated CleverSys forced swim test apparatus (CleverSys, Reston, VA) and investigators were unblinded to dosing solutions. Animals (n = 8-11/group) were randomly assigned to treatment with either vehicle (30% hydroxypropyl-β-cyclodextrin/70% citrate buffer, pH 4; 5 ml/kg, i.v.), CP-101,606 (3 mg/kg, i.v.) or BMS-986169 (0.3, 0.56, 1 or 3 mg/kg, i.v.) and 15 min later placed in plexiglass swim tanks (20 cm diameter, 40 cm height) filled with water up to a height of 20 cm at a temperature of 25 ± 1°C. In a separate study, mice were randomly assigned to treatment (n = 9-10/group) with either vehicle (0.9% saline; 10 ml/kg, i.v.) or ketamine (1, 3 or 10 mg/kg, i.v.) and tested 30 min after dosing. Swim tanks were positioned inside a box made of plastic and separated from each other by opaque plastic sheets to the height of cylinders. Individual animals were placed in one of the 3 swim tanks and behavior recorded in a 6 min testing session. The total immobility duration, defined as the time spent passively floating with only small movements necessary to keep the nose/head above water and remain afloat during the 6 min test, was measured using the automated CleverSys software. Results were analyzed by 1 way ANOVA followed by Dunnett's post-hoc test (GraphPad Prism v7.02). Upon completion of testing (~25

min after drug treatment) a subset of animals (n = 4/group) were euthanized by rapid decapitation and blood and brain samples collected for GluN2B occupancy and drug exposure measurements as previously described.

Novelty suppressed feeding (NSF) in mice

Studies to examine the effect of GluN2B NAM treatment on NSF were conducted at BBRC. Prior to treatment all mice were briefly (~1 min) placed in a restrainer to acclimatize them to the i.v. dosing conditions for 2 consecutive days. Animals were then randomly assigned to treatment (n = 12-15/group) with either CP-101,606 (10 mg/kg, i.v.), BMS-986163 (1, 3 or 10 mg/kg, i.v.) or their respective vehicles (25% hydroxypropyl-β-cyclodextrin or phosphate buffer, pH 7.4 respectively; 5 ml/kg, i.v.) and then food deprived for 21 h with water available *ad libitum*. On the following day (i.e. 24 h after treatment) individual mice were placed in a novel perspex arena (40 × 40 × 40 cm, Coulbourn instruments, Allentown, PA) covered on three sides with white paper with the 4th left transparent to enable behavioral evaluation. A light source was positioned on the top to produce a light intensity of ~1000 lux in the center of the arena. One food pellet (standard chow feed) was placed on the top of a 60 mm petri plate placed in the center of the arena. The session began with the animal placed in one corner of the arena facing away from the food pellet. The latency to begin eating the pellet (i.e. latency to feed) was recorded by an observer blinded to drug treatment. Feeding was defined as the mouse holding the food pellet with its forepaws and biting it and testing was terminated either when the mouse started to feed or after 6 min had elapsed. After evaluation in the novel arena, the mouse was transferred to its home cage and food consumption monitored for 30 min (home cage feeding). Results were

analyzed by either 2 tailed, unpaired t test (CP-101,606 versus vehicle) or 1 way ANOVA followed by Dunnett's post-hoc test (GraphPad Prism v7.02). Satellite groups of mice (n = 4/treatment) were dosed in parallel with the NSF subjects and plasma and brain samples collected 15 min later for exposure and GluN2B occupancy determinations.

During the initial pharmacological characterization of the NSF assay studies were conducted to examine the effect of ketamine treatment following intraperitoneal (i.p.) administration, a dosing route commonly used to examine the antidepressant-like effect of this agent. Subjects (n = 12-15/group) were treated with vehicle (milliQ water, 10 ml/kg) or ketamine (3, 10 or 30 mg/kg) and tested in the NSF assay 24 h later as described above.

Ex vivo hippocampal LTP in rats

Studies to examine the effects of GluN2B NAM treatment on hippocampal LTP were conducted by BMS. Rats were handled and acclimatized to the i.v. dosing restrainer for up to 5 min each day for 3 days prior to dosing. On the morning of drug treatment, rats were restrained and dosed via the tail vein by an investigator unblinded to treatment with either BMS-986169 (1 or 3 mg/kg) or vehicle (30% hydroxypropyl-β-cyclodextrin/70% citrate buffer; 2 ml/kg). Typically either 2 rats (one treated, one control) or 4 rats (2 treated, 2 control) were randomly assigned to treatment each day for subsequent LTP measurements 24 or 72 h later. Each dose of BMS-986169 or timepoint was examined as a separate study with independent vehicle-treated controls (n = 5-8/group). At the appropriate time point rats were rapidly decapitated and brain tissue removed and quickly submerged into ice-cold cutting solution containing 100 mM

JPET Fast Forward. Published on September 27, 2017 as DOI: 10.1124/jpet.117.242784
This article has not been copyedited and formatted. The final version may differ from this version.

sucrose, 60 mM NaCl, 3 mM KCl, 7 mM $MgCl_2$•$6H_2O$, 1.25 mM NaH_2PO_4, 0.5 mM $CaCl_2$, 5 mM D-glucose, 0.6 mM ascorbate and 28 mM $NaHCO_3$. The cerebellum and frontal cortex were removed and the brain cut down the midline. Transverse slices (350 µm) were cut from the middle of the hippocampal formation with a vibratome (Leica VT1000S, Leica Microsystems, Germany) in ice-cold cutting solution bubbled with 95% O_2/5% CO_2. Brain slices were transferred to a 50:50 mixture of cutting solution and aCSF containing 124 mM NaCl, 3 mM KCl, 1 mM $MgSO_4$•$7H_2O$, 1.25 mM NaH_2PO_4, 2 mM $CaCl_2$, 10 mM D-glucose, and 36 mM $NaHCO_3$ and oxygenated with 95% O_2/5% CO_2 at room temperature (26˚C) for 30 min. Slices were then switched to 100% aCSF and continued to be oxygenated with 95% O_2/5% CO_2 at 30˚C for at least 30 min of recovery. Up to 8 slices were recorded from simultaneously using a modified multi-slice recording configuration (Graef et al., 2013). Briefly, two separate tissue slice chambers, each with a capacity for 4 isolated tissue slices were perfused with warm (32-34˚C), oxygenated aCSF using a gravity perfusion system. A flow rate of 2 ml/min for each 4-slice recording chamber was regulated by maintaining a constant fluid level in a secondary solution chamber through the use of a solenoid valve (Harvard Apparatus), a float and an IR beam detector (NV-253SD, Med Associates). Four vehicle slices were placed in one of the 4-slice recording chambers and four slices from a rat treated with test agent were placed in the other 4-slice recording chamber, with the chambers used for each condition being alternated on subsequent experimental days. Once all slices were oriented in the recording chambers, custom-made recording and stimulating electrodes (0.2 µm diameter platinum/iridium wire) were positioned in the stratum radiatum (SR) layer of the CA1 region of the hippocampus. Field responses were

elicited with a single monophasic stimulation from two twisted wires (0.1 ms) every 20 s (3 Hz) using individual IsoFlex stimulus isolator units driven by a Master 8 stimulus generator (A.M.P.I.). The strength of each stimulus was adjusted to elicit 30–50% of the maximum response. Baseline signals were recorded for 20 min, then long-term potentiation (LTP) was induced by the following high frequency stimulation (HFS) protocol: 2 trains of 80 stimulations at 100 Hz at the same stimulus intensity, with a 60 s interval between trains. This HFS protocol was repeated two more times at 20 and 40 min following the first bout of HFS. Following this conditioning stimulus, a 1 h test period was recorded where responses were again elicited by a single stimulation every 20 s (3 Hz) at the same stimulus intensity. Signals were amplified with a differential amplifier and were digitized and sampled at 10 kHz with a DigiData 1440 (Molecular Devices), recorded using Clampex 10.0 acquisition software and analyzed with the Clampfit 10.0 software package (Molecular Devices). Data from all four slices from each animal (control and treated) on each experimental day were averaged to get mean LTP values for each subject. Only data from slices where the baseline responses were greater than 0.1 mV and did not vary by more than 10%, and demonstrated at least a 10% potentiation of the baseline response were used for analysis. These inclusion criteria were pre-specified prior to the LTP recordings and resulted in average values from 2-4 slices/subject. The total number of slices excluded from analysis across all studies were as follows: LTP amplitude: vehicle = 9/78 (11.5%), BMS-986169 = 9/79 (11.4%); LTP slope: vehicle = 8/78 (10.3%), BMS-986169 = 9/79 (11.4%). The number of slices excluded from analysis for individual studies were as follows: study 1: vehicle (24 h) = 1/27 slices, 3 mg/kg BMS-986169 (24 h) = 3/27 slices (slope) or 4/27 slices (amplitude);

study 2: vehicle (72 h) = 4/31 slices, 3 mg/kg BMS-986169 (72 h) = 4/32 slices; study 3: vehicle (24 h) = 3/20 slices (slope) or 4/20 slices (amplitude), 1 mg/kg BMS-986169 (24 h) = 2/20 slices (slope) or 1/20 slices (amplitude). One-tailed paired t-tests comparing corresponding test periods between control and treated animals were used to test for statistical significance.

Locomotor activity in mice

Studies to examine the effect of GluN2B NAM treatment on mouse locomotor activity were conducted at BBRC and performed using an automated LMA apparatus. All testing was conducted between 09:00-13:30 h in a dark room with low noise conditions and investigators were unblinded to dosing solutions. Mice were habituated to individual chambers (40 x 40 x 40 cm; Coulbourn Instruments, Allentown, PA) for 2 h and then randomly assigned to treatment. In an initial study the dose-response to ketamine was examined in mice (n = 8-9/group) treated with vehicle (milliQ water, 5 ml/kg i.v.) or ketamine (3, 10, 30 mg/kg i.v.). In the subsequent study mice (n = 7-8/group) were treated with either vehicle (25% hydroxy-β-cyclodextrin/75% water; 5 ml/kg, i.v.), ketamine (30 mg/kg, i.v.) or BMS-986169 (3, 10 or 30 mg/kg, i.v.). Animals were returned to the chamber and activity data acquired every 250 ms from the floor panel sensor and expressed as ambulatory distance (cm) recorded in 10 min time bins using TruScan 2.0 software. Results were analyzed by 2 way repeated measures (RM) ANOVA followed by Dunnett's post hoc analysis (GraphPad Prism v7.02). Separate satellite groups (n = 4/treatment) were dosed in parallel and plasma and brain tissue collected 15 min later to determine drug concentrations and GluN2B occupancy.

Abnormal behaviors in Cynomolgus Monkeys

Studies to examine the effect of GluN2B NAM treatment on spontaneous behaviors in monkeys were conducted by BMS. Prior to treatment baseline behavioral profiles were established by observing home cage behavior for 15 min per week for 3 weeks. Behaviors were evaluated using a 12 item behavioral checklist previously used to demonstrate psychotomimetic-like behaviors following treatment with amphetamine or ketamine in macaques (Castner and Goldman-Rakic 1999; Roberts et al., 2010; Supplemental Table 1). When a given behavior was observed, a mark was made in the appropriate time bin. Each study was organized using a Latin-Square design and the observer was blinded to treatment. A 5 min pre-dose observation was made 30 min before treatment with either vehicle (30% hydroxypropyl-β-cyclodextrin/70% water, 0.4 ml/kg, i.m.), (±)ketamine (1 mg/kg, i.m.) or BMS-986169 (1, 3 or 5.6 mg/kg, i.m.) and behavior evaluated 0-5, 5-10, 10-15, 30-35 and 60-65 min post treatment (n = 8). To examine a higher dose of 10 mg/kg BMS-986169 a second blinded study was conducted using a Latin-Square design and a 2-injection protocol whereby 2 x 0.4 ml/kg injections were given to achieve a total dose of 10 mg/kg BMS-986169, 1 mg/kg ketamine or two injections of vehicle (n = 8). The dose of ketamine used for comparison was selected from a separate study showing a dose-dependent increase in behavior after ketamine administration (n = 12). Behaviors were summed over the entire session and expressed in terms of change from pre-injection baseline. Composite measures of 'all abnormal behaviors' (behaviors 2+4+6+7+10+11; Supplemental Table 1) and 'hallucinatory/dissociative' (behaviors 7+11; Supplemental Table 1) were calculated and analyzed by 1 way RM ANOVA followed by Dunnett's post-hoc test (GraphPad Prism v7.02). On completion of the evaluation subjects were placed in a primate restraint chair

and a plasma sample (~75 min post dose) collected from the saphenous vein for measurement of drug concentrations.

Cognitive Impairment in Cynomolgus Monkeys

Studies to examine the effect of GluN2B NAM treatment on cognitive performance were conducted at BMS using a list delayed match to sample (list-DMS) procedure described previously (Weed et al., 2016). Subjects (n = 9) had received prior treatment with other pharmacological agents and were given at least a 2 month drug free period prior to the start of these studies. During the procedure animals were seated in restraint chairs and placed within a sound attenuated chamber containing a touch sensitive computer monitor controlled by the Monkey CANTAB (Cambridge Neuropsychological Testing Automated Battery) software; (Lafayette Instruments, Lafayette, IN). Following correct responses, a dispenser delivered 190 mg banana flavored pellets (Bioserv, Frenchtown, PA). Animals were first trained to proficiency on the standard CANTAB DMS task in which an abstract stimulus is presented in the 'sample' phase and, after a memory delay, the sample stimulus + 3 distracter stimuli are presented in the 'choice' phase. Animals then progressed to a list-DMS procedure in which three different sample stimuli are presented first followed by their choice phases which occur sequentially based on their respective memory delays. Thus the 3 trials are nested within the longest memory delay thereby reducing the overall session length. The memory delays used in this study were 2, 20 and 45 s. Completion of the list was followed by a 10 s screen blank after which a new list was presented for a total of 20 lists in each test session. During both the sample and choice phases the subject had 5 s to respond to the stimulus otherwise the trial was considered an omission. If the omission was in the sample

phase, the choice phase for that sample stimulus was not presented but the timing of sample and choice phases for other stimuli remain unchanged. All subjects were habituated to receiving injections prior to testing. Evaluation of performance after vehicle (25% hydroxypropyl-β-cyclodextrin/75% water, 0.4 ml/kg i.m.) treatment occurred prior to, during and at the end of the dose-response function (total of 4 vehicle determinations). The effect of BMS-986169 treatment was tested twice weekly (Monday and Thursday) with baseline performance sessions on Tuesday and Friday. On test days the cohort was divided roughly in half and one half received a given dose of BMS-986169 and the other half received a different dose. Drug doses were thus administered in a mixed order across test days and across subjects by investigators unblinded to treatment. In the first study the effect of BMS-986169 (0.1, 0.3, 1 or 3 mg/kg, i.m.) administered 30 min prior to testing was examined to determine the dose-effect relationship. In a follow up study vehicle or 1 mg/kg BMS-986169 was administered 3 or 5 h prior to testing to examine the time course of the effect. List-DMS test sessions were ~30 min long and on completion blood samples were collected from the saphenous vein for analysis of plasma drug concentrations. Sample collection times, therefore, correspond to 1 h post-dose for the dose-response study and 3.5 or 5.5 h for the time course study. Plasma and CSF drug concentrations were also investigated after dosing with BMS-986169 (0.3-5.6 mg/kg, i.m.) in a separate cohort of cynomolgus monkeys previously implanted with vascular and CSF lumbar access ports (n = 2/group). Blood samples were collected into K2EDTA tubes on ice, plasma separated by centrifugation at 1330g for 10 min and plasma and CSF samples stored at -80°C until analyzed.

The primary measure for these studies was performance accuracy expressed as the percentage of correct trials (% accuracy = [correct trials]/[(correct trials + errors)] x 100). Secondary measures included i) latency to respond in the choice phase (ms between onset of stimulus presentation and touching of monitor) and ii) percent task completed (trials with a response in both sample and choice phase/trials presented). Omissions were not included in the percent correct measure, but contributed to percent task completed. Percent correct accuracy was analyzed by 2 way RM ANOVA followed by Dunnett's post-hoc test. For the time course study, performance after vehicle treatment was similar regardless of the pretreatment time (0.5, 3 or 5 h) and the average was therefore used in the analysis. Latencies to respond in the choice phase (averaged across delays) and percent task completed for the entire session were analyzed by one way RM-ANOVA followed by Dunnett's post hoc test. In addition, for the long delay condition, the difference between performance after vehicle and drug treatment was calculated for each for each subject as follows: difference = % correct at long delay[drug treatment] - % correct at long delay[vehicle treatment]. All statistical analysis were conducted using GraphPad Prism (v7.02).

Quantitative EEG studies in Cynomolgus Monkeys

Studies to examine the effect of GluN2B NAM treatment on the qEEG response were conducted by BMS using methods described previously (Keavy et al., 2016). Six cynomolgus monkeys served as subjects for the qEEG studies and each had been used previously in pharmacological studies, with a drug-free period of at least one month prior to testing. Subjects were surgically implanted under isoflurane anesthesia with radio-telemetry transmitters (Konigsberg Instruments, Inc., Monrovia, CA) attached to

two sets of EEG leads placed over the dura: one set with leads over the frontal cortex (with a reference over parietal cortex; roughly F6-P6 in the 10-20 system) and the second set with leads over the auditory cortex (roughly C6-CP6 in the 10-20 system). Buprenorphine (0.01-0.03 mg/kg, i.m.) was administered after surgery and for a further 2-3 days BID with extended treatment as needed if subjects showed signs of discomfort. After full recovery (approximately 3-4 weeks), the implanted radio-telemetry device was tested to ensure a good EEG signal and suitable subjects enrolled in the study. On each test day, prior to the start of qEEG recordings, subjects were seated in a primate restraint chair and an i.v. catheter placed in a saphenous vein for drug administration. Animals were allowed to acclimate to a quiet testing chamber outfitted with an antenna to receive telemeter signals and a camera to monitor the animal during the session. After a 20 min baseline recording, animals were treated with either vehicle (0.9% saline, 0.4 ml/kg i.v.) or BMS-986163 (0.12, 0.36 or 1.2 mg/kg, i.v.) by investigators unblinded to treatment and the qEEG measured for a further 90 min. The i.v. catheter was removed at the end of the session and animals were tested once weekly with treatments assigned using a Latin Square design. Analog signals from the telemeters were digitized at 1,000 Hz by Powerlab DAQ systems (ADInstruments, Colorado Springs, CO). Raw EEG waveforms were Fourier transformed using a Han (Cosine Bell) window with 50% overlap between data blocks and an FFT block size of 1024. Overall total power (0.5-55 Hz) as well as power within the different frequency bands was recorded for delta (0.5-4 Hz), theta (4-9 Hz), alpha (9-13 Hz), beta 1 (13-19 Hz), beta 2 (20-30 Hz) and gamma (30-55 Hz) bandwidths. The relative power (power in a band/overall total power) was determined as the average value from one min bins

across the 90 min session and analyzed by 2 way RM ANOVA followed by Holm-Sidak post-hoc test (GraphPad Prism v7.02). Area under the curve (AUC) over the entire 90 min period for each power band was calculated from the time course data and analyzed by RM ANOVA followed by Dunnett's post-hoc test (GraphPad Prism v7.02). Finally, using the AUC results, the Cohen's d estimate of effect size was calculated using unpaired statistics (http://www.uccs.edu/~lbecker/).

Plasma and CSF drug concentrations were also investigated after dosing with BMS-986163 (1.2 mg/kg, i.v.) cynomolgus monkeys previously implanted with vascular and CSF lumbar access ports (n = 2/time point). Sample collection, processing and storage was as previously described.

Quantification of BMS-986169 and BMS-986163 in samples from *in vivo* studies

For exposure analysis of BMS-986169 and BMS-986163 in plasma, brain, and CSF, rats and monkeys were dosed and samples collected as described. BMS-986163 was stabilized *ex vivo* by collecting blood samples into tubes containing 4% K_2EDTA dissolved in 1 M phosphate buffer pH 7.4 (5% of the blood volume) and maintained at 4°C. Plasma was gathered within 15 min of blood collection and stored at -80°C until analysis. For brain samples, tissue was homogenized and diluted with blank plasma. CSF samples were prepped in the same manner as plasma. An aliquot of 50 µL of calibration standard or study sample (plasma/tissue/CSF) was added to 200 µL of acetonitrile containing internal standard (Ro-25-6981 at 100 nM) and transferred to a Strata protein precipitation filter plate (Phenomenex, Torrance, CA). Plates were vortexed on a plate shaker for 5 min at 300 rpm, centrifuged at 4000 rpm for 5 min, and the eluent was collected into a 96 well collection plate (Waters Corporation, Milford,

USA). A volume of 4 µL was injected for LC-MS/MS analysis. LC-MS/MS analysis was performed on a Waters Acquity UPLC (Waters Corp., Milford, MA) interfaced to a Sciex API4000 triple quadrupole mass spectrometer (Toronto, Canada) equipped with a Turboionspray source. The source temperature was set at 550°C and the ionspray voltage was set to 4.5 kV. Samples were maintained at 10°C for the duration of the analysis. Separations were performed on a Waters Acquity BEH C18 (2.1 x 50 mm, 1.7 µm) column maintained at 60°C. The mobile phase, which consisted of 0.1% (v/v) formic acid in water (A) and 0.1% (v/v) formic acid in acetonitrile (B), was delivered at a flow rate of 700 µL/min. Separation was achieved using a gradient elution starting at 95% aqueous mobile phase and going to 95% organic mobile phase. Nitrogen was used as nebulizer and auxiliary gas with a pressure and flow rate of 80 psi and 7 L/min, respectively. Data acquisition utilized selected reaction monitoring (SRM) operating mode. Standard curves used for quantification were fitted with linear regression weighted by reciprocal concentration $1/x^2$. Data and chromatographic peaks were quantified using Analyst version 1.4.2 software.

Results

BMS-986169 potently inhibits [^{3}H]Ro 25-6981 binding in vitro

Saturation binding experiments showed that [^{3}H]Ro 25-6981 labeled a single population of receptors in membranes prepared from rat forebrain, cynomolgus monkey frontal cortex or human frontal cortex with Kd values of 2.23 nM (n = 3), 0.93 nM (n = 1) and 1.99 nM (n = 2), respectively. BMS-986169, CP-101,606 and MK-0657 potently and

JPET Fast Forward. Published on September 27, 2017 as DOI: 10.1124/jpet.117.242784
This article has not been copyedited and formatted. The final version may differ from this version.

completely displaced [^{3}H]Ro 25-6981 specific binding in all species (Table 1; Supplemental Figures 1 and 2).

BMS-986169 selectively inhibits GluN2B receptor function

To demonstrate that BMS-986169 inhibits GluN2B receptor function, electrophysiological recordings were made in Xenopus oocytes expressing human GluN1a/GluN2B receptors. Application of BMS-986169 produced a concentration dependent inhibition of glutamate/glycine activated currents; the IC_{50} value was 24.1 nM (95% confidence limits (CL) 20.1 - 28.9) determined from a 7 point concentration response curve (n = 3-5/concentration) (Figure 2). In comparison, the IC_{50} values determined following 15 min incubation with CP-101,606 or Ro 25-6981 were 10.6 nM (95% CL 7.7 - 14.6) and 9.3 nM (95% CL 8.4 - 10.4), respectively (Figure 2). BMS-986169 showed minimal inhibition of glutamate/glycine activated currents at other NMDA receptor subtypes; the mean ± S.D. inhibition at 3 µM was -2.4 ± 2.6%, 8.6 ± 6.4% and 7 ± 3.8% at human GluN1a/GluN2A, GluN1a/GluN2C or GluN1a/GluN2D receptors, respectively (n = 2-3). BMS-986169 was also examined in a broad panel of *in vitro* assays at 40 additional pharmacological targets with no additional activity of relevance identified (Supplemental Table 2). Finally, BMS-986169 showed weak functional inhibition at hERG channels; the IC_{50} determined by patch clamp electrophysiology in HEK293 cells expressing hERG was 28.4 µM.

IV administration of BMS-986169 or BMS-986163 achieves high levels of GluN2B receptor occupancy in rat brain

Intravenous administration of BMS-986169 produced a dose-dependent increase in *ex vivo* GluN2B occupancy determined in rat brain homogenates 15 min after dosing; the dose achieving 50% occupancy was 0.22 mg/kg (95% CL 0.13 - 0.37) with 97% occupancy achieved at the highest dose tested (3 mg/kg; Figure 3A). Treatment with the phosphate prodrug, BMS-986163, also produced a dose-dependent increase in GluN2B occupancy determined 15 min after i.v. dosing in rats (Figure 3A). Again maximal occupancy was achieved at 3 mg/kg BMS-986163 (101%) and the dose achieving 50% occupancy was 0.42 mg/kg (95% CL 0.28 - 0.61). As expected, GluN2B occupancy was closely correlated with the total plasma concentration of BMS-986169 following dosing of either BMS-986169 or BMS-986163 (Figure 3B). These results confirm that the prodrug is rapidly converted to the parent drug after i.v. administration and are consistent with other pharmacokinetic studies showing little to no detectable levels of prodrug in the systemic circulation. Brain tissue concentrations of BMS-986169 also showed a strong relationship with GluN2B occupancy (Supplemental Table 3; Supplemental Figure 3A); the average brain tissue/total plasma concentration ratio across all GluN2B occupancy studies was 3. Investigation of the occupancy time course after dosing with 3 mg/kg i.v. BMS-986169 showed that peak occupancy (~93%) was maintained for up to 30 min and then declined rapidly to a level of 57% 2 h after treatment (Figure 3C). Analysis of BMS-986169 concentrations in plasma (total and free drug concentration), brain tissue and CSF collected from these subjects showed a strong relationship between drug exposure and occupancy in all compartments (Figure 3D; Supplemental Table 3). BMS-986169 was detected in CSF at levels similar to the free plasma drug concentration at all time points examined (Supplemental Figure 3B).

JPET Fast Forward. Published on September 27, 2017 as DOI: 10.1124/jpet.117.242784
This article has not been copyedited and formatted. The final version may differ from this version.

The CSF concentration to achieve 50% GluN2B occupancy was 3.5 nM and was consistent with the *in vitro* GluN2B binding affinity. In addition, GluN2B occupancy, predicted from CSF concentrations and the rat *in vitro* GluN2B binding Ki, was similar to the measured occupancy in these subjects (Supplemental Figure 3C). It should be noted that BMS-986169 shows poor oral bioavailability in rats; the oral bioavailability determined after oral dosing with 5 mg/kg BMS-986169 or the prodrug BMS-986163 was 2.5% and 1.7% respectively.

BMS-986163 functionally inhibits NMDA receptors after IV dosing in rats

Intravenous administration of the phosphate prodrug, BMS-986163 dose-dependently inhibited *in vivo* [^{3}H]MK-801 binding with a maximal 41% inhibition achieved at 10 mg/kg (Figure 4A). Satellite groups of rats, receiving jugular vein injections of the same BMS-986163 dosing solutions, showed 97% GluN2B occupancy at 10 mg/kg and an Occ50 dose of 0.55 mg/kg (95% CL 0.2 - 1.47) (Figure 4A). Further examination of the [^{3}H]MK-801 binding response confirmed that inhibition saturates at ~40% after treatment with BMS-986163 (mean ± S.E.M. % inhibition 15 min after dosing: 10 mg/kg = 38.4 ± 1.2; 30 mg/kg = 43.6 ± 2.7). Inhibition of [^{3}H]MK-801 binding was also time-dependent; the maximal inhibition achieved after dosing with 3 mg/kg BMS-986163 was 37% and occurred at 15 min post-treatment (Figure 4B). Thereafter, inhibition of [^{3}H]MK-801 binding declined rapidly over time and was negligible (6% inhibition) by 2 h post-treatment (Figure 4B). Again, GluN2B occupancy determined in satellite groups was high ($\geq$ 89%) for the first 30 min after dosing and then declined rapidly to a level of 28% 2 h after treatment (Figure 4B). The relationship between total plasma and brain BMS-

JPET Fast Forward. Published on September 27, 2017 as DOI: 10.1124/jpet.117.242784
This article has not been copyedited and formatted. The final version may differ from this version.

986169 concentrations and GluN2B occupancy from these combined studies was similar to previous results (Supplemental Table 3; Supplemental Figure 4).

BMS-986169 reduces immobility in the mouse FST

Treatment with BMS-986169 produced a significant, dose-dependent decrease in immobility (ANOVA: $F(5,53) = 3.547$; $P = 0.0077$) (Figure 5A) in mice tested in the FST assay. The minimum effective dose was 1 mg/kg which achieved an average total plasma BMS-986169 concentration and GluN2B occupancy of 268 nM and 73.3%, respectively, determined immediately after completion of the test (Supplemental Table 4). Decreased immobility was also seen in mice treated with CP-101,606 (3 mg/kg, i.v.) which achieved a mean (± S.E.M.) GluN2B occupancy of 85 ± 0.45%. As expected, BMS-986169 produced a dose- and exposure-dependent increase in *ex vivo* GluN2B receptor occupancy; the dose achieving 50% occupancy was 0.4 mg/kg (95% CL 0.16 - 0.82) and the total plasma and brain drug concentrations achieving 50% occupancy were 102 nM and 404 nM respectively (Supplemental Figure 5; Supplemental Table 3). The average BMS-986169 brain tissue/total plasma concentration ratio in mice was 4. A dose-dependent decrease in immobility was also seen after i.v. ketamine administration ($F(3,34) = 5.212$, $P = 0.0045$) which was significant at doses of 3 and 10 mg/kg and similar in magnitude to the effects seen with BMS-986169 (Figure 5B).

BMS-986163 reduces NSF 24 h after IV dosing in mice

Treatment with BMS-986163 produced a dose-dependent decrease in the latency to feed in a novel environment determined 24 h after dosing in mice (ANOVA: $F(3,52) = 4.635$, $P = 0.006$) (Figure 5C). A similar reduction in latency was also observed in CP-

101,606 treated animals (unpaired t test: P = 0.0255) (Figure 5C). Home cage food consumption, measured on completion of testing in the NSF assay, was not significantly different from vehicle-treated subjects in mice treated with BMS-986163 (ANOVA: F(3,52) = 1.976, P = 0.1291) or CP-101,606 (unpaired t test: P = 0.9731) (Figure 5D). Measurement of GluN2B occupancy, 15 min after dosing in satellite groups of mice, showed that 101% occupancy was achieved at both 3 and 10 mg/kg BMS-986163 (Supplemental Table 4). The mean ± S.E.M. GluN2B occupancy determined 15 min after CP-101,606 (10 mg/kg, i.v.) administration was 92 ± 1%.

The effect of intravenous ketamine administration has not been tested however intraperitoneal (i.p.) dosing was examined during our initial characterization of the NSF assay. Ketamine significantly reduced the latency to feed in the novel environment (ANOVA: F(3,51) = 3.788, P = 0.0158) 24 h after administration of 10 and 30 mg/kg i.p. with no effect observed on home cage food consumption (ANOVA: F(3,51) = 1.749, P = 0.1687) (Supplemental Figure 6).

BMS-986169 enhances ex vivo hippocampal LTP 24 h after dosing in rats

Recordings from hippocampal slices taken from vehicle-treated rats showed that application of HFS increased both the amplitude and the slope of the fEPSP response compared to baseline recordings consistent with the induction of LTP. A single administration of BMS-986169 (3 mg/kg, i.v.) produced a robust enhancement of *ex vivo* hippocampal LTP measured 24 h after dosing (Figure 6). This elevation was apparent for both the amplitude (Figure 6 A, B) and the slope (Figure 6 C, D) of the fEPSP response with a significant enhancement over baseline observed following application of all three HFS stimuli. The elevation of LTP was dose related with a small, but

significant elevation of the fEPSP slope observed 24 h after treatment with BMS-986169 (1 mg/kg, i.v.) (Supplemental Table 5). Finally, the enhancement of LTP was time dependent and was no longer observed 72 h after dosing with 3 mg/kg BMS-986169 (Supplemental Table 5).

BMS-986169 has marginal effects on LMA in mice

Treatment with ketamine produced a significant increase in LMA that lasted 50 min after dosing with 10 or 30 mg/kg (treatment effect: $F(3,31) = 19.81$, $P<0.0001$; time effect: $F(11,341) = 99.19$, $P<0.0001$; interaction: $F(33,341) = 8.232$, $P<0.0001$) (Figure 7A). In comparison, treatment with BMS-986169 had marginal effects on LMA (treatment effect: $F(4,31) = 9.97$, $P<0.0001$; time effect: $F(11,341) = 62.62$, $P<0.0001$; interaction ($F(44,341) = 6.76$, $P<0.0001$) (Figure 7B). Treatment with 3 mg/kg BMS-986169 had no effect on LMA at any time point. At higher doses, a small but significant increase was observed in the first 10 min after dosing which was substantially lower than the ketamine response (Figure 7B). A small increase was also observed at the 50-60 min time point in mice treated with 30 mg/kg. All doses of BMS-986169 were associated with high levels of GluN2B occupancy (range = 96.4 - 99.7%) determined 15 min after i.v. dosing in satellite groups of mice (Supplemental Table 4).

BMS-986169 does not produce ketamine-like dissociative/hallucinogenic-like effects in cynomolgus monkeys

In a previous study i.m. ketamine administration produced a dose-dependent increase in the incidence of abnormal and dissociative/hallucinogenic-like behaviors; the dose of 1 mg/kg was chosen as the comparator for further investigation (Supplemental Figure

7). Two independent studies were conducted to examine the effects of intramuscular administration of BMS-986169 on spontaneous behaviors in cynomolgus monkeys; the first examined BMS-986169 at doses of 1, 3 or 5.6 mg/kg and the second examined BMS-986169 at the dose of 10 mg/kg. Results from repeated measures ANOVA showed a significant effect of treatment on the incidence of abnormal behaviors (study 1: $F(4,28) = 12.06$, $P<0.0001$; study 2: $F(2,14) = 14.43$, $P = 0.0004$) and dissociative/hallucinogenic behaviors (study 1: $F(4,28) = 6.533$, $P = 0.0008$; study 2: $F(2,14) = 11.08$, $P = 0.0013$). Dunnett's post-hoc analysis showed that the incidence of these behaviors was significantly increased following ketamine (1 mg/kg, i.m.) treatment whereas BMS-986169 had no effect at any dose tested (Figure 8). Analysis of total plasma BMS-986169 concentrations on completion of testing (~75 min post-treatment) showed dose-dependent exposure ranging from 620 - 10,260 nM (Supplemental Table 6).

BMS-986169 transiently impairs working memory in cynomolgus monkeys

Vehicle-treated monkeys performing the list-DMS task showed a significant decrease in performance accuracy as the delay between the initial presentation of the stimulus and the choice phase increased (mean ± S.E.M. % accuracy: short delay = 95.6 ± 1.3%; medium delay = 74 ± 4.1%***; long delay = 63.7 ± 4.6% ***; one way RM ANOVA ($F(2,16) = 33.3$, $P<0.0001$) followed by Dunnett's post hoc test compared to short delay). Intramuscular injection of BMS-986169 produced a significant dose- and delay-dependent decrease in performance accuracy in subjects tested 30 min after dosing (treatment: $F(4,32) = 39.21$; $P<0.0001$; delay: $F(2,16) = 116.2$, $P<0.0001$; interaction: $F(8,64) = 8.533$; $P<0.0001$). Further post-hoc analysis showed that BMS-986169 had no

JPET Fast Forward. Published on September 27, 2017 as DOI: 10.1124/jpet.117.242784
This article has not been copyedited and formatted. The final version may differ from this version.

effect on performance accuracy at short delays at any dose tested (Figure 9A). In contrast, a significant impairment in accuracy was observed at both the medium and long delays in subjects treated with 1 mg/kg and 3 mg/kg BMS-986169 (Figure 9A). The lack of effect at short delays indicates that performance of the task *per se* is not altered by drug treatment. Consistent with these results treatment with BMS-986169 did not alter % task completion indicating no effect on motivation to perform the task at any dose (Supplemental Figure 8A). While a significant increase in latency to respond was seen at the highest dose, this increase (~300 ms) is only a minor slowing of response time (Supplemental Figure 8B). The effect of treatment with 1 mg/kg BMS-986169 on performance accuracy was also time dependent (treatment: $F(3,24) = 18.7$, $P<0.0001$; delay: $F(2,16) = 103.1$, $P<0.0001$; interaction: $F(6,48) = 8.112$, $P<0.0001$) with maximal impairment observed 30 min post-dose and full recovery achieved by 5 h after treatment (Figure 9C). Again there was no effect on % task completion or response latency consistent with a selective memory impairment (Supplemental Figure 8 C, D). Across both studies the degree of impairment, as represented by the difference in the % accuracy from vehicle treatment at the long delay condition, was related to total plasma BMS-986169 concentrations measured on completion of testing in experimental subjects (Figure 9B, D; Supplemental Table 6) with large impairments seen at plasma concentrations $\geq$483 nM. Investigation of plasma exposures in a separate group of subjects confirmed that total plasma BMS-986169 concentrations are stable across the duration of the list-DMS task (i.e. 30-60 min post dose; Supplemental Figure 9A). CSF concentrations of BMS-986169 increased in a dose-dependent manner ranging from 18.5 - 79 nM at 30 min post-dose (Supplemental Figure 9B). The predicted GluN2B

occupancy, calculated using CSF concentrations and the monkey *in vitro* GluN2B binding Ki value (4.2 nM), ranged from 81.5 - 95% across the dose range examined (Supplemental Figure 9B).

BMS-986163 alters qEEG power band distribution in cynomolgus monkeys

Intravenous administration of BMS-986163 produced robust and dose-related changes in the qEEG power distribution in the beta 1, alpha and delta power bands. Analysis of time course data showed that all doses of BMS-986163 reduced the relative power in the beta1 power band (Supplemental Table 7). At the highest dose (1.2 mg/kg) a significant increase in relative power in the delta band and decrease in the alpha band were also observed (Supplemental Table 7). Time course results show that treatment effects emerged rapidly and were sustained throughout the 90 min recording period (Figure 10A; Supplemental Figures 10,11 and 12). Analysis of results expressed as the area under the relative power curve (AUC) confirmed these results except for the low dose (0.12 mg/kg) effect on beta 1 (Figure 10B; Supplemental Table 8; Supplemental Figure 13). Cohen's d analysis showed that the relative power changes produced at the highest dose of BMS-986163 were moderate (>0.5) to large (>0.8) with effect sizes of 0.77 (delta), -0.88 (alpha) and -1.01 (beta 1), respectively (Figure 10C). Investigation of plasma exposure, in separate subjects dosed with BMS-986163 (1.2 mg/kg, i.v.), showed that maximal total plasma BMS-986169 concentrations were achieved within 5 min of dosing confirming rapid conversion of the prodrug to parent (Figure 10D) in monkeys. Consistent with these results, the prodrug concentrations in 5 min plasma samples were negligible and below the assay limits of quantification (<156 nM). CSF concentrations of BMS-986169 were stable over the 90 min qEEG recording period

(Figure 10D) and associated with a high level of predicted GluN2B occupancy of 97-98%.

Discussion

Selective inhibition of the GluN2B receptor subtype has been proposed as a strategy to deliver novel therapeutics with ketamine-like antidepressant efficacy and improved tolerability. Using well established *in vitro* approaches (Mutel et al., 1998; Malherbe et al., 2003; Risgaard et al., 2013; Ng et al., 2008) BMS-986169 was identified as a novel agent with high affinity for the GluN2B ATD allosteric site (Ki = 4-6 nM) that potently and selectively inhibits GluN2B receptor function (IC_{50} = 24.1 nM). BMS-986169 showed negligible activity in a broad assay panel consisting of 40 additional targets. Importantly, BMS-986169 weakly inhibited hERG channels (IC_{50} = 28.4 µM), an off-target liability that has been challenging to address in chemical scaffolds targeting the GluN2B NAM site (Müller et al., 2011; Brown et al., 2011; Layton et al., 2011).

The *in vivo* characterization of BMS-986169 and the phosphate prodrug BMS-986163 focused on: 1) confirmation of occupancy and functional inhibition of GluN2B receptors, 2) testing in assays of antidepressant drug-like effects and side effects and 3) testing on translational measures that can be investigated in healthy humans. GluN2B occupancy in rodents was measured by *ex vivo* [^{3}H]Ro 25-6981 binding (Fernandes et al., 2015) and showed a dose-dependent increase that fully saturated at doses $\geq$3 mg/kg. Occupancy was tightly correlated with exposure and occupancy/exposure relationships were similar after i.v. dosing with BMS-986169 or BMS-986163 confirming rapid and effective cleavage of the prodrug. Functional inhibition of GluN2B receptors was demonstrated by inhibition of *in vivo* [^{3}H]MK-801 binding (Fernandes et al., 2015).

JPET Fast Forward. Published on September 27, 2017 as DOI: 10.1124/jpet.117.242784
This article has not been copyedited and formatted. The final version may differ from this version.

[^{3}H]MK-801 is a radiotracer that labels all NMDA receptor subtypes present in an open conformational state. The assay can be used to show both direct binding site competition following treatment with other NMDA receptor open channel blockers or binding inhibition due to the functional effects of agents acting at other modulatory sites (Murray et al., 2000; Fernandes et al., 2015). Specifically, the conformational change produced by binding to the GluN2B allosteric site closes channels containing the GluN2B subunit, prevents [^{3}H]MK-801 from accessing its binding site in the channel pore and reduces [^{3}H]MK-801 binding. Previous studies have shown that GluN2B NAMs maximally inhibit [^{3}H]MK-801 binding by ~60% suggesting that GluN2B containing NMDA receptors represent 60% of the total NMDA receptor population labeled *in vivo* (Fernandes et al., 2015). In a similar manner, treatment with BMS-986163 also inhibited [^{3}H]MK-801 binding in rats confirming functional NMDA receptor inhibition *in vivo*. However, in contrast to other agents, the maximal inhibition achieved at doses fully occupying the GluN2B NAM binding site was ~40% suggesting a subpopulation of GluN2B containing receptors that are less sensitive to functional inhibition by BMS-986169 *in vivo*. Lower inhibition could reflect functional differences in discrete brain regions expressing GluN2B receptors; the current homogenate assay does not address this question and GluN2B functional inhibition is not detectable using *ex vivo* [^{3}H]MK-801 autoradiography (Lord et al., 2013). Different receptor subtypes, namely diheteromeric GluN1/GluN2B and triheteromeric GluN1/GluN2A/GluN2B receptors, may also be involved since differences in functional potency and maximal inhibition at tri- versus di- heteromeric receptors have been reported for CP-101,606 (Hansen et al., 2014). Additional studies, including *in vivo* approaches such as pharmacological

magnetic resonance imaging may provide further insight into this interesting result (Chin et al., 2011).

To provide evidence of antidepressant drug-like effects we first tested BMS-986169 in the mouse FST, a simple behavioral assay sensitive to many antidepressant drug classes and multiple NMDA receptor agents (Porsolt et al., 1977; Trullas and Skolnick, 1990; Pilc et al., 2013). As expected, BMS-986169 reduced immobility 15 min after dosing consistent with results for other GluN2B NAMs (Li et al., 2010; Kiselycznyk et al., 2015; Refsgaard et al., 2017). We next showed that BMS-986169 robustly elevated *ex vivo* hippocampal LTP measured 24 h after treatment. As evidence of synaptic strengthening, this finding is consistent with the hypothesis that rapid acting antidepressants enhance synaptic plasticity (Wohleb et al., 2017) and with results for ketamine and the structurally distinct GluN2B NAM, CP-101,606, in this assay (Burgdorf et al., 2013; Graef et al., 2015). The effect is thought to arise from increased expression of synaptic proteins such as GluR1 and PSD95 and at least two mechanisms downstream of NMDA receptor inhibition may be involved; i) disinhibition of pyramidal glutamate neurons leading to activity-dependent BDNF release and activation of ERK/AKT/mTORC1 signaling and/or 2) activity-independent blockade of extra-synaptic, postsynaptic NMDA receptors leading to reduced eEF2 kinase activity, decreased eEF2 phosphorylation and de-suppression of BDNF and synaptic protein translation (Miller et al., 2016; Murrough et al., 2017). Finally, we showed that BMS-986163 reduced latency to feed in the NSF assay, a model of stress-induced anxiety that is sensitive to chronic, but not acute treatment with classical antidepressant agents (Dulawa and Hen 2005). Importantly we demonstrated efficacy 24 h after dosing, a result consistent with the

sustained efficacy seen after acute ketamine treatment in this assay (Iijima et al. 2012). With respect to target engagement, LTP and NSF results suggest that high levels of GluN2B occupancy, sustained for a critical duration, are necessary to deliver efficacy 24 h after dosing. Robust LTP enhancement was seen at 3 mg/kg which achieves ~95% peak occupancy and maintains ≥80% occupancy for ~1 h. Efficacy in NSF was seen only at 10 mg/kg, while peak occupancy was saturated at doses ≥ 3 mg/kg suggesting the duration of occupancy is important. This initial characterization suggests that BMS-986169/BMS-986163 has potential as a rapid acting antidepressant and supports progression to further testing in more complex animal models and investigation of the molecular mechanisms involved (Ramaker and Dulawa, 2017).

While BMS-986169 showed low potential to produce ketamine-like hyperactivity or abnormal behaviors, impaired working memory was observed in monkeys performing the CANTAB list-DMS task. We chose i.m. dosing for these studies to ensure stable plasma levels during the 30 min testing session and to facilitate demonstration of the effect. Importantly this impairment was transient, fully resolving by 5 h post-dose and was closely related to plasma exposures with subsequent pharmacokinetic modeling predicting a more rapid resolution after i.v. administration. This profile is similar to other GluN2B NAMs tested in this model (Weed et al., 2016) and consistent with electrophysiology studies showing that persistent activation of dorsolateral prefrontal cortical delay neurons is dependent upon GluN2B receptors in monkeys performing working memory tasks (Wang et al., 2013; Wang and Arnsten 2015). The temporal differences between the working memory and hippocampal LTP effects should be noted; working memory deficits coincide with the primary pharmacological effect i.e.

GluN2B receptor inhibition, whereas enhanced 24 h LTP is measured at a time when downstream events leading to synaptic strengthening have occurred. Given the overlapping exposures and (predicted) occupancy across these assays the separation of doses providing antidepressant-like effects from those producing transient cognitive impairment within the first hour(s) of dosing may not be possible for this mechanism.

The present results raise important questions about the optimal GluN2B NAM candidate profile. From this perspective both intravenous (CP-101,606) and oral agents (CERC-301, aka MK-0657) have been examined in patients. In the case of CP-101,606, a single i.v. infusion improved depression symptoms in a small cohort of TRD patients with minimal dissociative effects (Preskorn et al., 2008). In contrast, while CERC-301 initially appeared promising (Ibrahim et al., 2012) a recent study showed that treatment with 8 mg daily was not effective in severely depressed TRD patients (www.Cerecor.com). It is possible that target engagement is inadequate at this dose of CERC-301 since preclinical results suggest that exposures reported in MDD patients receiving a 4-8 mg titration (Ibrahim et al., 2012) only briefly (~2 h) achieve levels predicted to deliver ~50% occupancy (Addy et al., 2009). Management of cognitive impairment may be difficult for oral agents with a long pharmacokinetic half-life if human results confirm the high target engagement requirement for antidepressant effects suggested by preclinical studies. Thus an i.v. agent may be preferred since exposure can be tightly controlled to deliver transient, high levels of GluN2B occupancy while enabling monitoring for resolution of any transient cognitive impairment within a clinical setting.

To facilitate the progression of BMS-986163 we examined effects on the qEEG. Previous studies have shown robust qEEG power band changes in monkeys treated with GluN2B NAMs (Keavy et al., 2016) and BMS-986163 produced the same pattern of response. As an approach, changes in qEEG related measures for NMDA receptor antagonists generally align well across species and, while not tested here, other measures such as auditory evoked potentials also have translational utility for GluN2B NAMs (Nagy et al., 2016). Such approaches may provide valuable information; for example, the sustained qEEG effect was not anticipated after i.v. dosing but is likely explained by the relatively stable CSF levels of BMS-986169 during the recording window. Thus, qEEG related measures provide a non-invasive way to monitor target engagement in humans and potentially aide the optimization of i.v. infusion regimens.

In conclusion, the present results support the further investigation of BMS-986163, the phosphate prodrug of the novel GluN2B NAM BMS-986169, as an i.v. agent with potential for a rapid antidepressant effect.

Acknowledgements

We would like to acknowledge Keely Walsh, Sharon Aborn, James Brennan and Margaret Batchelder for veterinary science assistance and study support; Michelle Nophsker for drug formulation support; David Luchetti for dosing and sample collection support; Peng Li, Dauh-Rurng Wu and Richard Rampulla for chemistry synthesis and scale-up support.

Authorship Contributions

Participated in research design: Bristow, Gulia, Weed, Srikumar, Y.-W. Li, Graef, Naidu, Kumar, Sivarao, Keavy, Shields, J. Li, Zhang, Mathur, Ramarao, Vikramadithyan, Thangathirupathy, Warrier, Bronson, Olson, Macor, Albright, King, Thompson, Marcin and Sinz.

Conducted experiments: Gulia, Weed, Srikumar, Graef, Naidu, Sanmathi, Aher, Bastia, Paschapur, Kalidindi, Kumar, Molski, Pieschl, Fernandes, Newberry, Bookbinder, Polino, Keavy, Newton, Shields, Simmermacher, Kempson, J. Li, Sinha, Ramarao, Thangathirupathy, Warrier and Thompson.

Contributed new reagents or analytical tools: Brown, Sivarao, Shields, Kempson, Kallem, Thangathirupathy, Warrier, King and Thompson.

Performed data analysis: Bristow, Gulia, Weed, Srikumar, Y.-W. Li, Graef, Naidu, Sanmathi, Aher, Paschapur, Kalidindi, Kumar, Pieschl, Fernandes, Sivarao, Keavy, Shields, Simmermacher, J. Li, Ramarao, Thangathirupathy, Warrier and Thompson.

Wrote or contributed to the writing of the manuscript: Bristow, Gulia, Weed, Shields, Simmermacher, Olson and Sinz.

References

Addy C, Assaid C, Hreniuk D, Stroh M, Xu Y, Herring WJ, Ellenbogen A, Jinnah HA, Kirby L, Leibowitz MT, Stewart RM, Tarsy D, Tetrud J, Stoch SA, Gottesdiener K and Wagner J (2009) Single-dose administration of MK-0657, an NR2B-selective NMDA antagonist, does not result in clinically meaningful improvement in motor function in patients with moderate Parkinson's disease. J Clin Pharmacol **49**: 856-864.

Berman RM, Cappiello A, Anand A, Oren DA, Heninger GR, Charney DS and Krystal JH (2000) Antidepressant effects of ketamine in depressed patients. Biol Psychiatry **47**: 351-354.

Brown DG, Maier DL, Sylvester MA, Hoerter TN, Menhaji-Klotz E, Lasota CC, Hirata LT, Wilkins DE, Scott CW, Trivedi S, Chen T, McCarthy DJ, Maciag CM, Sutton EJ, Cumberledge J, Mathisen D, Roberts J, Gupta A, Liu F, Elmore CS, Alhambra C, Krumrine JR, Wang X, Ciaccio PJ, Wood MW, Campbell JB, Johansson MJ, Xia J, Wen X, Jiang J, Wang X, Peng Z, Hu T and Wang J (2011) 2,6-Disubstituted pyrazines and related analogs as NR2B site antagonists of the NMDA receptor with antidepressant activity. Bioorg Med Chem Lett **21**: 3399-3403.

Burgdorf J, Zhang XL, Nicholson KL, Balster RL, Leander JD, Stanton PK, Gross AL, Kroes RA and Moskal JR (2013) GLYX-13, a NMDA receptor glycine-site functional partial agonist, induces antidepressant-like effects without ketamine-like side effects. Neuropsychopharmacology **38**: 729-742.

Castner SA and Goldman-Rakic PS (1999) Long-lasting psychotomimetic consequences of repeated low-dose amphetamine exposure in rhesus monkeys. Neuropsychopharmacology **20**: 10-28.

Chin CL, Upadhyay J, Marek GJ, Baker SJ, Zhang M, Mezler M, Fox GB and Day M (2011) Awake rat pharmacological magnetic resonance imaging as a translational pharmacodynamic biomarker: metabotropic glutamate 2/3 agonist modulation of ketamine-induced blood oxygen level dependence signals. J Pharmacol Exp Ther **336**: 709-715.

Dulawa SC and Hen R (2005) Recent advances in animal models of chronic antidepressant effects: the novelty-induced hypophagia test. Neurosci Biobehav Rev **29**: 771-783.

Fava M (2006) Pharmacological approaches to the treatment of residual symptoms. J Psychopharmacol **20**: 29-34.

Fernandes A, Wojcik T, Baireddy P, Pieschl R, Newton A, Tian Y, Hong Y, Bristow L and Li YW (2015) Inhibition of in vivo [(3)H]MK-801 binding by NMDA receptor open channel blockers and GluN2B antagonists is rats and mice. Eur J Pharmacol **766**: 1-8.

Gaynes BN, Warden D, Trivedi MH, Wisniewski SR, Fava M and Rush AJ (2009) What did STAR*D teach us? Results from a large scale, practical, clinical trial for patients with depression. Psychiatr Serv **60**: 1439-1445.

Graef JD, Newberry K, Newton A, Pieschl R, Shields E, Luan FN, Simmermacher J Luchetti D, Schaeffer E, Li YW, Kiss L and Bristow LJ (2015) Effect of acute NR2B

antagonist treatment on long-term potentiation in the rat hippocampus. Brain Res **1609**: 31-39.

Graef JD, Wei H, Lippiello PM, Bencherif M and Fedorov N (2013) Slice XVIvo^{TM}: a novel electrophysiology system with the capability for 16 independent brain slice recordings. J Neurosci Methods **212**: 228-233.

Greenberg PE, Fournier AA, Sisitsky T, Pike CT and Kessler RC (2015) The economic burden of adults with major depressive disorder in the United States (2005 and 2010). J Clin Psychiatry **76**: 155-162.

Hansen KB, Ogden KK, Yuan H and Traynelis SF (2014) Distinct functional and pharmacological properties of triheteromeric GluN1/GluN2A/GluN2B NMDA receptors. Neuron **81**: 1084-1096.

Ibrahim L, DiazGranados N, Jolkovsky L, Brutsche N, Luckenbaugh DA, Herring WJ, Potter WZ and Zarate CA Jr (2012) A randomized, placebo-controlled, crossover pilot trial of the oral selective NR2B antagonist MK-0657 in patients with treatment-resistant major depressive disorder. J Clin Psychopharmacol **32**: 551-557.

Iijima M, Fukumoto K and Chaki S (2012) Acute and sustained effects of a metabotropic glutamate 5 receptor antagonist in the novelty-suppressed feeding test. Behav Brain Res **235**: 287-292.

Keavy D, Bristow LJ, Sivarao DV, Batchelder M, King D, Thangathirupathy S, Macor JE and Weed MR (2016) The qEEG signature of selective NMDA NR2B negative allosteric modulators; a potential translational biomarker for drug development. PLoS One doi: 10.1371/journal.pone.0152729.

Kiselycznyk C, Jury NJ, Halladay LR, Nakazawa K, Mishina M, Sprengel R, Grant SG, Svenningsson P and Holmes A (2015) NMDA receptor subunits and associated signaling molecules mediating antidepressant-related effects of NMDA-GluN2B antagonism. Behav Brain Res **287**: 89-95.

Layton ME, Kelly MJ 3rd and Rodzinak KJ (2006) Recent advances in the development of NR2B subtype-selective NMDA receptor antagonists. Curr Top Med Chem **6**: 697-709.

Layton ME, Kelly MJ 3rd, Rodzinak KJ, Sanderson PE, Young SD, Bednar RA, Dilella AG, McDonald TP, Wang H, Mosser SD, Fay JF, Cunningham ME, Reiss DR, Fandozzi C, Trainor N, Liang A, Lis EV, Seabrook GR, Urban MO, Yergey J and Koblan KS (2011) Discovery of 3-substituted aminocyclopentanes as potent and orally bioavailable NR2B subtype-selective NMDA antagonists. ACS Chem Neurosci **2**: 352-362.

Lener MS, Kadriu B and Zarate CA Jr (2017) Ketamine and beyond: Investigations into the potential of glutamatergic agents to treat depression. Drugs **77**: 381-401.

Li N, Lee B, Liu RJ, Banasr M, Dwyer JM, Iwata M, Li XY, Aghajanian G and Duman RS (2010) mTOR-dependent synapse formation underlies the rapid antidepressant effects of NMDA antagonists. Science **329**: 959-964.

Lord B, Wintmolders C, Langlois X, Nguyen L, Lovenberg T and Bonaventure P (2013) Comparison of the ex vivo receptor occupancy profile of ketamine to several NMDA receptor antagonists in mouse hippocampus. Eur J Pharmacol **715**: 21-25.

Maeng S, Zarate CA Jr, Du J, Schloesser RJ, McCammon J, Chen G and Manji HK (2008) Cellular mechanisms underlying the antidepressant effects of ketamine: role of

alpha-amino-3-hydroxy-5-methylisoxazole-4-propionic acid receptors. Biol Psychiatry **63**: 349-352.

Malherbe P, Mutel V, Broger C, Perin-Dureau F, Kemp JA, Neyton J, Paoletti P and Kew JN (2003) Identification of critical residues in the amino terminal domain of the human NR2B subunit involved in the RO 25-6981 binding pocket. J Pharmacol Exp Ther **307**: 897-905.

McClintock SM, Husain MM, Wisniewski SR, Nierenberg AA, Stewart JW, Trivedi MH, Cook I, Morris D, Warden D and Rush AJ (2011) Residual symptoms in depressed outpatients who responded by 50% but do not remit to antidepressant medication. J Clin Psychopharmacol **31**: 180-186.

Miller OH, Moran JT and Hall BJ (2016) Two cellular hypothesis explaining the initiation of ketamine's antidepressant actions: Direct inhibition and disinhibition. Neuropharmacology **100**: 17-26.

Miller OH, Yang L, Wang CC, Hargroder EA, Zhang Y, Delpire E and Hall BJ (2014) GluN2B-containing NMDA receptors regulate depression-like behavior and are critical for the rapid antidepressant actions of ketamine. eLife doi: 10.7554/eLife.03581.

Mony L, Kew JN, Gunthorpe MJ and Paoletti P (2009) Allosteric modulators of NR2B-containing NMDA receptors: molecular mechanisms and therapeutic potential. Br J Pharmacol **157**: 1301-1317.

Müller A, Höfner G, Renukappa-Gutke T, Parsons CG and Wanner KT (2011) Synthesis of a series of γ-amino alcohols comprising an N-methyl isoindoline moiety and their evaluation as NMDA receptor antagonists. Bioorg Med Chem Lett **21**: 5795-5799.

Murray F, Kennedy J, Hutson PH, Elliot J, Huscroft I, Mohnen K, Russel MG and Grimwood S (2000) Modulation of [3H]MK-801 binding to NMDA receptors in vivo and in vitro. Eur J Pharmacol **397**: 263-270.

Murrough JW, Abdallah CG and Mathew SJ (2017) Targeting glutamate signaling in depression: progress and prospects. Nat Rev Drug Discov **16**: 472-486.

Mutel V, Buchy D, Klingelschmidt A, Messer J, Bleuel Z, Kemp JA and Richards JG (1998) In vitro binding properties in rat brain of [3H]Ro 25-6981, a potent and selective antagonist of NMDA receptors containing NR2B subunits. J Neurochem **70**: 2147-2155.

Nagy D, Stoiljkovic M, Menniti FS and Hajós M (2016) Differential effects of an NR2B NAM and ketamine on synaptic potentiation and gamma synchrony: relevance to rapid-onset antidepressant activity. Neuropsychopharmacology **41**: 1486-1494.

Ng FM, Geballe MT, Snyder JP, Traynelis SF and Low CM (2008) Structural insights into phenylethanolamines high-affinity binding site in NR2B from binding and molecular modeling studies. Mol Brain doi: 10.1186/1756-6606-1-16.

Paykel ES, Ramana R, Cooper Z, Hayhurst H, Kerr J and Barocka A (1995) Residual symptoms after partial remission: an important outcome in depression. Psychol Med **25**: 1171-1180.

Pilc A, Wierońska JM and Skolnick P (2013) Glutamate-based antidepressants: preclinical psychopharmacology. Biol Psychiatry **73**: 1125-1132.

Popp S, Behl B, Joshi JJ, Lanz TA, Spedding M, Schenker E, Jay TM, Svenningsson P, Caudal D, Cunningham JI, Deaver D and Bespalov A (2016) In search of the

mechanisms of ketamine's antidepressant effects: How robust is the evidence behind the mTOR activation hypothesis? F1000Research doi: 10.12688/f1000research.8236.1.

Porsolt RD, Bertin A and Jalfre M (1977) Behavioral despair in mice: a primary screening test for antidepressants. Arch Int Pharmacodyn Ther **229**: 327-336.

Preskorn SH, Baker B, Kolluri S, Menniti FS, Krams M and Landen JW (2008) An innovative design to establish proof of concept of the antidepressant effects of the NR2B subunit selective N-methyl-D-aspartate antagonist, CP-101,606, in patients with treatment-refractory major depressive disorder. J Clin Psychopharmacol **28**: 631-637.

Ramaker MJ and Dulawa SC (2017) Identifying fast-onset antidepressants using rodent models Mol Psychiatry **22**: 656-665.

Refsgaard LK, Pickering DS and Andreasen JT (2017) Investigation of antidepressant-like and anxiolytic-like actions and cognitive and motor side effects of four N-methyl-D-aspartate receptor antagonists in mice. Behav Pharmacol **28**: 37-47.

Risgaard R, Nielsen SD, Hansen KB, Jensen CM, Nielsen B, Traynelis SF and Clausen RP (2013) Development of 2'-substituted (2S,1'R,2'S)-2-(carboxycyclopropyl)glycine analogues as potent N-methyl-d-aspartic acid receptor agonists. J Med Chem **56**: 4071-4081.

Roberts BM, Shaffer CL, Seymour PA, Schmidt CJ, Williams GV and Castner SA (2010) Glycine transporter inhibition reverses ketamine-induced working memory deficits. Neuroreport **21**: 390-394.

Trullas R and Skolnick P (1990) Functional antagonists at the NMDA receptor complex exhibit antidepressant actions. Eur J Pharmacol **185**: 1-10.

Ustün TB, Ayuso-Mateos JL, Chatterji S, Mathers C and Murray CJ (2004) Global burden of depressive disorders in the year 2000. Br J Psychiatry **184**: 386-392.

Wang M and Arnsten AF (2015) Contribution of NMDA receptors to dorsolateral prefrontal cortical networks in primates. Neurosci Bull **31**: 191-197.

Wang M, Yang Y, Wang CJ, Gamo NJ, Jin LE, Mazer JA, Morrison JH, Wang XJ and Arnsten AF (2013) NMDA receptors subserve persistent neuronal firing during working memory in dorsolateral prefrontal cortex. Neuron **77**: 736-749.

Weed MR, Bookbinder M, Polino J, Keavy D, Cardinal RN, Simmermacher-Mayer J, Cometa FN, King D, Thangathirupathy S, Macor JE and Bristow LJ (2016) Negative allosteric modulators selective for the NR2B subtype of the NMDA receptor impair cognition in multiple domains. Neuropsychopharmacology **41**: 568-577.

Weed MR, Taffe MA, Polis I, Roberts AC, Robbins TW, Koob GF, Bloom FE and Gold LH (1999) Performance norms for a rhesus monkey neuropsychological testing battery: acquisition and long-term performance. Brain Res Cogn Brain Res **8**: 185-201.

Wohleb ES, Gerhard D, Thomas A and Duman RS (2017) Molecular and cellular mechanisms of rapid-acting antidepressants ketamine and scopolamine. Curr Neuropharmacol **15**: 11-20.

Footnotes

This work was supported by Bristol-Myers Squibb Company. At the time these studies were conducted all authors were either employees of Bristol-Myers Squibb Company or employees of the Biocon Bristol-Myers Squibb Research Center (BBRC). Some authors own Bristol-Myers Squibb Company stock. Additionally some authors are inventors on patents related to the subject matter.

Reprint requests should be directed to: Larry Marcin, Bristol-Myers Squibb Company, 5 Research Parkway, Wallingford, CT 06492. Email: lawrence.marcin@bms.com

Figure legends

Figure 1 Chemical structures of BMS-986169 and the phosphate prodrug BMS-986163.

Figure 2 BMS-986169 inhibits glutamate/glycine currents in xenopus oocytes expressing human GluN1a/GluN2B receptors. A) Representative recording showing inhibition of 50 µM glutamate + 30 µM glycine currents following application of 100 nM BMS-986169. B) Concentration response curve for inhibition of glutamate/glycine activated currents. Each point shows the mean ± S.E.M. % inhibition following 15 min incubations with either BMS-986169 (n = 3-5/concentration), CP-101,606 (n = 1-4/concentration) or Ro 25-6981 (n = 1-2/concentration).

Figure 3 Ex vivo GluN2B occupancy in rat brain following tail vein administration of BMS-986169 or the phosphate prodrug BMS-986163. A) Occupancy dose response and B) total plasma concentration/occupancy relationship determined 15 min after BMS-986169 or BMS-986163 treatment. C) Occupancy time course and D) relationsip between occupancy and total plasma, free plasma, brain tissue and CSF BMS-986169 concentration in rats treated with 3 mg/kg BMS-986169. Results are presented as the mean ± S.E.M. % GluN2B occupancy (n = 4-5/dose) or exposure/occupancy results for individual subjects.

Figure 4 Inhibition of *in vivo* [^{3}H]MK-801 binding and relationship to *ex vivo* GluN2B occupancy in rats treated with the phosphate prodrug BMS-986163. A) Dose response determined 15 min after i.v. dosing and B) time course determined in rats treated with 3 mg/kg (i.v.). Results are presented as the mean ± S.E.M. % inhibition of [^{3}H]MK-801 binding (n = 4/group) or % GluN2B occupancy (n = 3/group).

Figure 5 Effect of i.v. administration of A) BMS-986169 or B) ketamine on immobility in the mouse FST assay. Results are presented as the mean ± S.E.M. immobility duration determined A) 15 min after treatment with BMS-986169 or CP-101,606 (CP; 3 mg/kg, i.v.; n = 8-11/group) or B) 30 min after treatment with ketamine (n = 9-10/group). Results were analyzed by ANOVA followed by Dunnett's post hoc test; **P<0.01, *P<0.05 compared to vehicle (Veh). Effect of i.v. administration of BMS-986163 or CP-101,606 (CP; 10 mg/kg) on C) novelty suppressed feeding and D) home cage feeding determined 24 h after dosing in mice (n = 12-15/group). Results are presented as the mean ± S.E.M. latency to feed in the novel environment or quantity of food consumed in the home cage during a 30 min period beginning immediately after testing in the novel environment. Treatment effects were compared to their respective vehicle (Veh) by either unpaired t test (CP-101,606 versus Veh-1) or ANOVA followed by Dunnett's post hoc test (BMS-986163 versus Veh-2); *P<0.05, **P<0.01.

Figure 6 BMS-986169 (3 mg/kg, i.v.) enhances *ex vivo* hippocampal LTP 24 h after dosing in rats. A) and C) Time course of the normalized fEPSP amplitude (A) or slope (C). B) and D) % Increase over baseline of the fEPSP amplitude (B) or slope (D) during the last 5 min of recording following each HFS application. Results are presented as the mean ± S.E.M. (n = 7/group). Results at each HFS (B and D) were analyzed by one-tailed, paired t test; *P<0.05 compared to vehicle.

Figure 7 A) Increased LMA after i.v. ketamine treatment in mice (n = 8-9/group). B) Effect of BMS-986169 (i.v.) or ketamine (30 mg/kg, i.v.) on LMA in mice (n = 7-8/group). Results are presented as the mean ± S.E.M. ambulatory distance in 10 min time bins recorded

for 2 h after dosing. Results were analyzed by 2 way RM ANOVA followed by Dunnett's post hoc test; *P<0.05, **P<0.01, *** P<0.001 compared to vehicle.

Figure 8 BMS-986169 does not produce abnormal or dissociative/hallucinogenic-like behaviors in cynomolgus monkeys (n = 8). Results are presented as the mean ± S.E.M. total score for A) all abnormal behaviors or B) dissociative/hallucinogenic behaviors observed up to 65 min after i.m. dosing with vehicle, ketamine (Ket; 1 mg/kg, i.m.) or BMS-986169 (1 - 10 mg/kg). Results were analyzed by RM ANOVA followed by Dunnett's post-hoc test; **P<0.01, *** P<0.001 compared to vehicle.

Figure 9 BMS-986169 produces a transient impairment in working memory after i.m. dosing in cynomolgus monkeys (n = 9). Effect on list-DMS accuracy determined A) 30 min after dosing with BMS-986169 (0.1 - 3 mg/kg, i.m.) or C) at various time points after dosing with 1 mg/kg (i.m.) BMS-986169. Results are presented as the mean ± S.E.M. % correct responses at short, medium or long delays and were analyzed by 2 way RM ANOVA followed by Dunnett's post-hoc test; ***P<0.001 compared to vehicle. Relationship between total plasma BMS-986169 concentration and impairment at long delays determined B) 30 min after dosing with BMS-986169 and D) at various time points after dosing with 1 mg/kg BMS-986169. Results are presented as the mean ± S.E.M. difference from vehicle in % correct responses at the long delay condition or the mean + S.D. total plasma BMS-986169 concentration (n = 7-9/group).

Figure 10 Robust effects on the qEEG power band distribution after i.v. treatment with BMS-986163 in cynomolgus monkeys (n = 6). A) Time course of the effect of 1.2 mg/kg i.v. BMS-986163 on relative power in the beta 1 power band. Results are presented as the mean ± S.E.M. relative power in 1 min time bins and were analyzed by 2 way RM

ANOVA followed by Holm-Sidak post-hoc test. B) Effect of BMS-986163 on relative power in the beta 1 power band. Results are presented as the mean ± S.E.M. area under the beta 1 relative power curve (AUC) and were analyzed by RM ANOVA followed by Dunnett's t test; *P<0.05, **P<0.01, ***P<0.001 compared to vehicle. C) Treatment effect size for changes in the qEEG power band distribution. Results show the Cohen's d values, calculated using the relative power AUC, for each power band after treatment with BMS-986169. Statistics correspond to results from the AUC analysis as described in B). D) Mean (± S.D.) total plasma and CSF concentration of BMS-986169 measured in separate subjects after i.v. administration of 1.2 mg/kg BMS-986163 (n = 2/group).

JPET Fast Forward. Published on September 27, 2017 as DOI: 10.1124/jpet.117.242784
This article has not been copyedited and formatted. The final version may differ from this version.

Tables

Table 1 Displacement of [^{3}H]Ro 25-6981 binding to native GluN2B receptors in membranes prepared from rat forebrain, cynomolgus monkey frontal cortex or human frontal cortex.

Compound	Rat Mean Ki ± S.D.	Monkey Mean Ki ± S.D.	Human Mean Ki ± S.D.
BMS-986169	4.03 ± 1.39 nM (n = 13)	4.2 ± 0.8 nM (n = 3)	6.3 ± 1.5 nM (n = 3)
CP-101,606	6.96 ± 0.56 nM (n = 3)	2.2 ± 0.5 nM (n = 4)	3.1 ± 0.9 nM (n = 4)
MK-0657	2.52 ± 0.42 nM (n = 3)	3.2 ± 0.5 nM (n = 3)	4.4 ± 1.4 nM (n = 3)

Figures

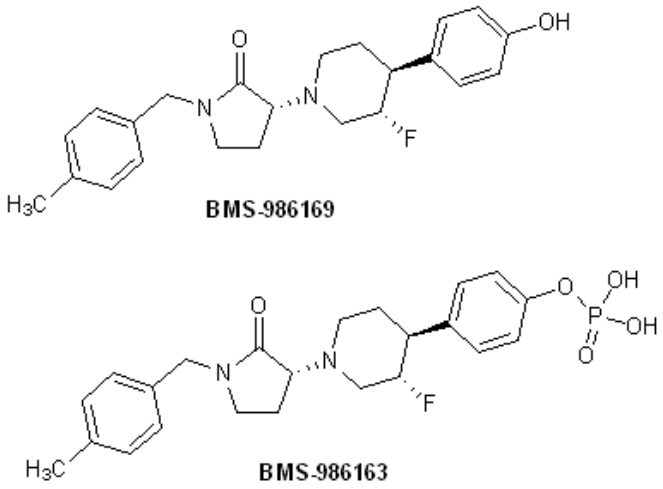

Figure 1

JPET Fast Forward. Published on September 27, 2017 as DOI: 10.1124/jpet.117.242784
This article has not been copyedited and formatted. The final version may differ from this version.

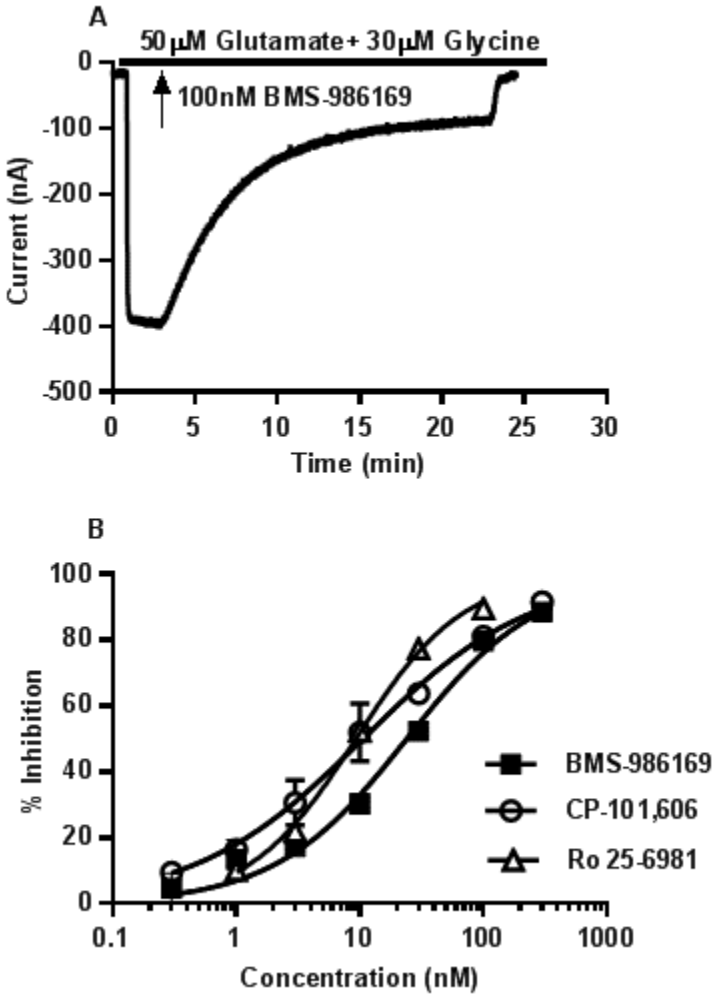

Figure 2

JPET Fast Forward. Published on September 27, 2017 as DOI: 10.1124/jpet.117.242784
This article has not been copyedited and formatted. The final version may differ from this version.

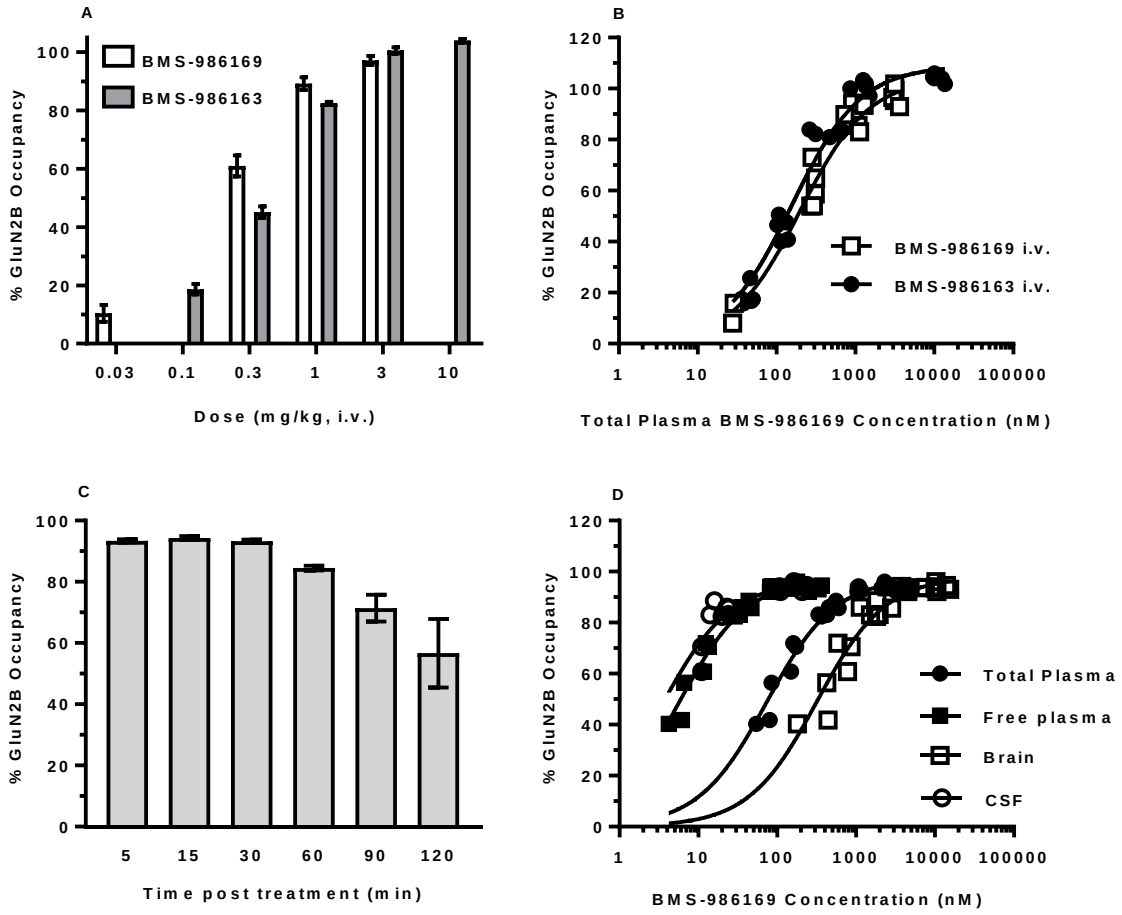

Figure 3

JPET Fast Forward. Published on September 27, 2017 as DOI: 10.1124/jpet.117.242784
This article has not been copyedited and formatted. The final version may differ from this version.

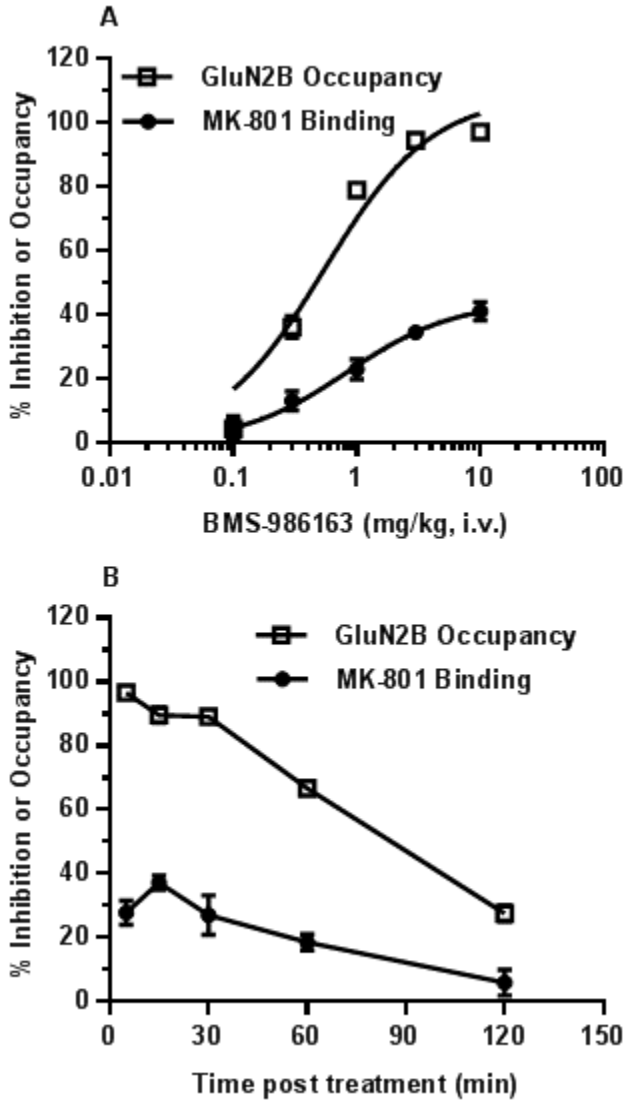

Figure 4

JPET Fast Forward. Published on September 27, 2017 as DOI: 10.1124/jpet.117.242784
This article has not been copyedited and formatted. The final version may differ from this version.

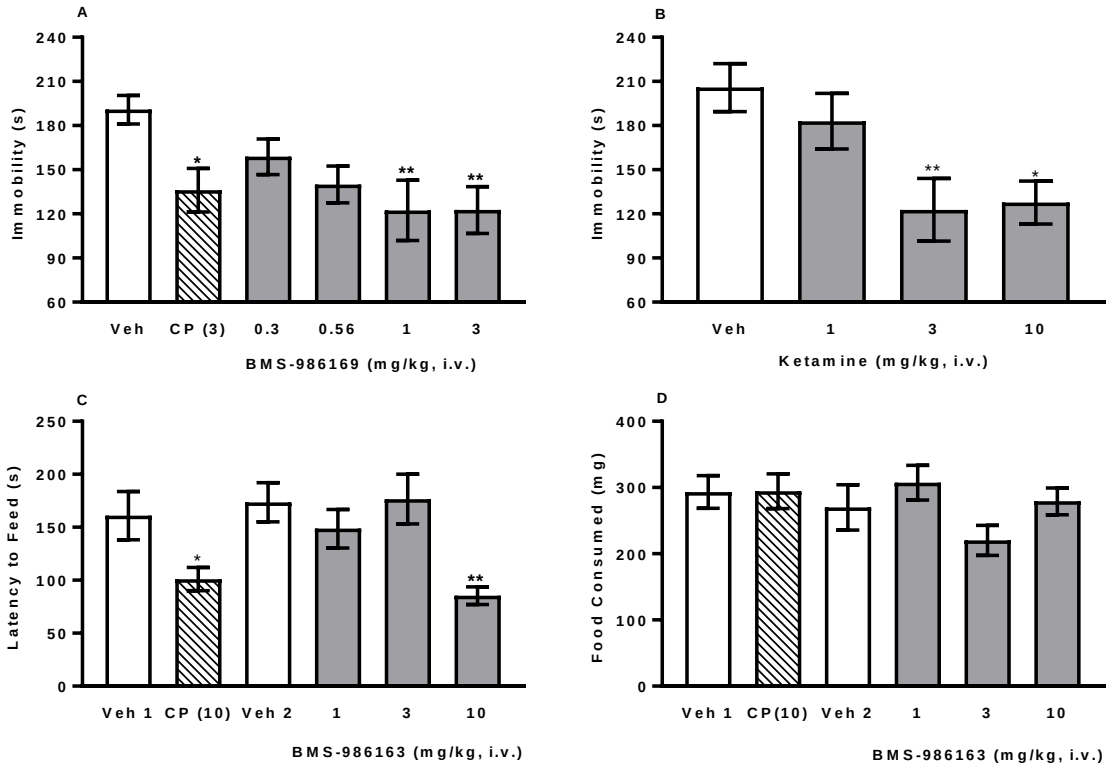

Figure 5

JPET Fast Forward. Published on September 27, 2017 as DOI: 10.1124/jpet.117.242784
This article has not been copyedited and formatted. The final version may differ from this version.

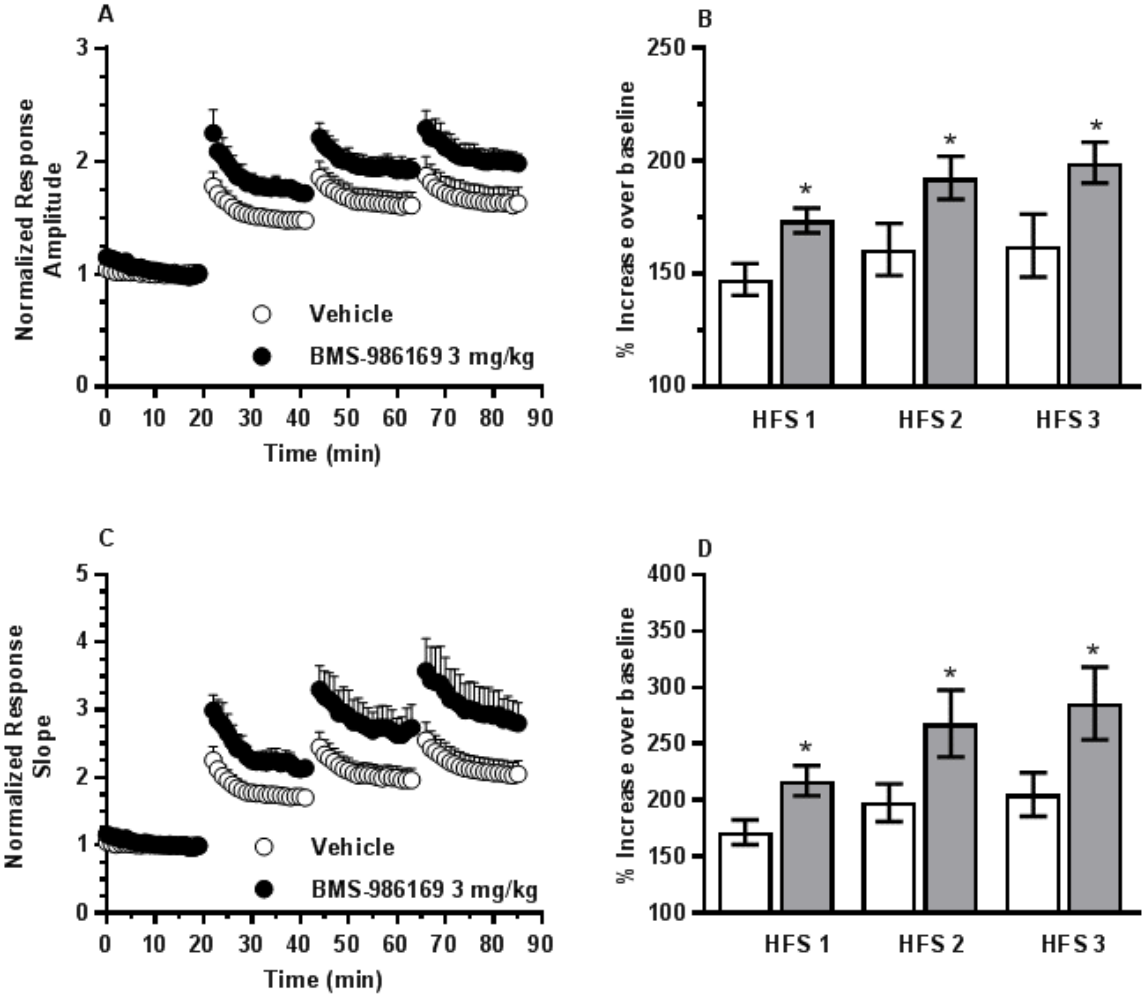

Figure 6

JPET Fast Forward. Published on September 27, 2017 as DOI: 10.1124/jpet.117.242784
This article has not been copyedited and formatted. The final version may differ from this version.

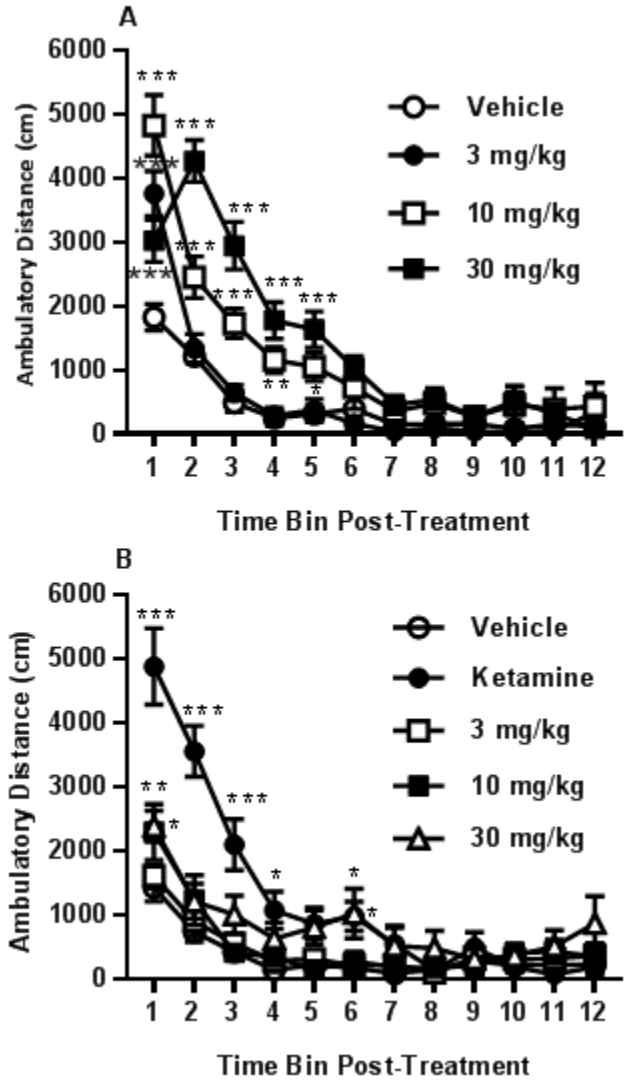

Figure 7

JPET Fast Forward. Published on September 27, 2017 as DOI: 10.1124/jpet.117.242784
This article has not been copyedited and formatted. The final version may differ from this version.

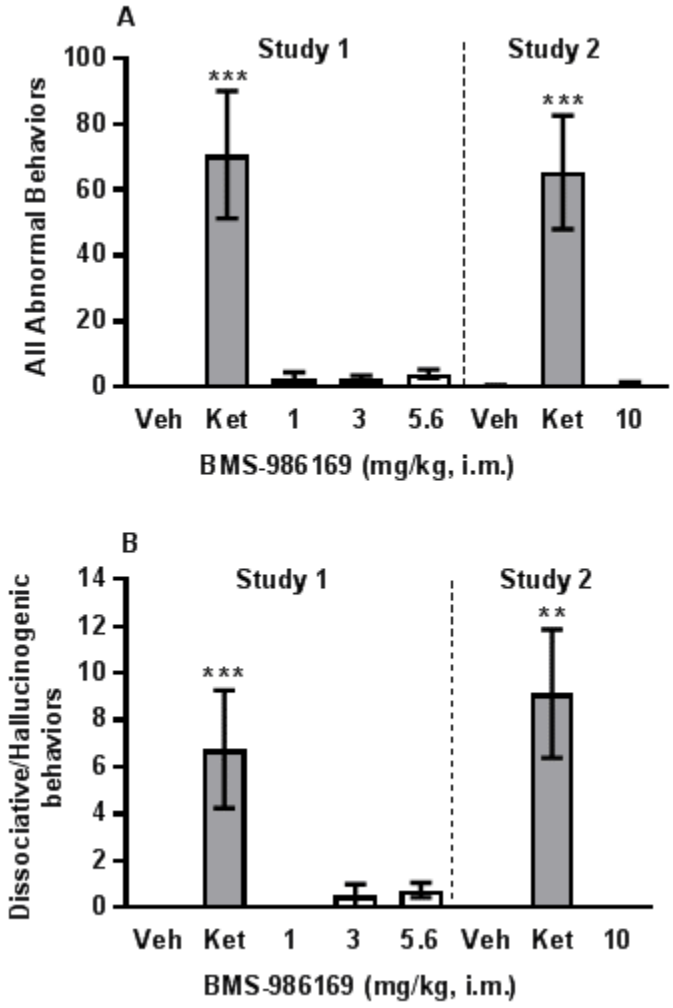

Figure 8

JPET Fast Forward. Published on September 27, 2017 as DOI: 10.1124/jpet.117.242784
This article has not been copyedited and formatted. The final version may differ from this version.

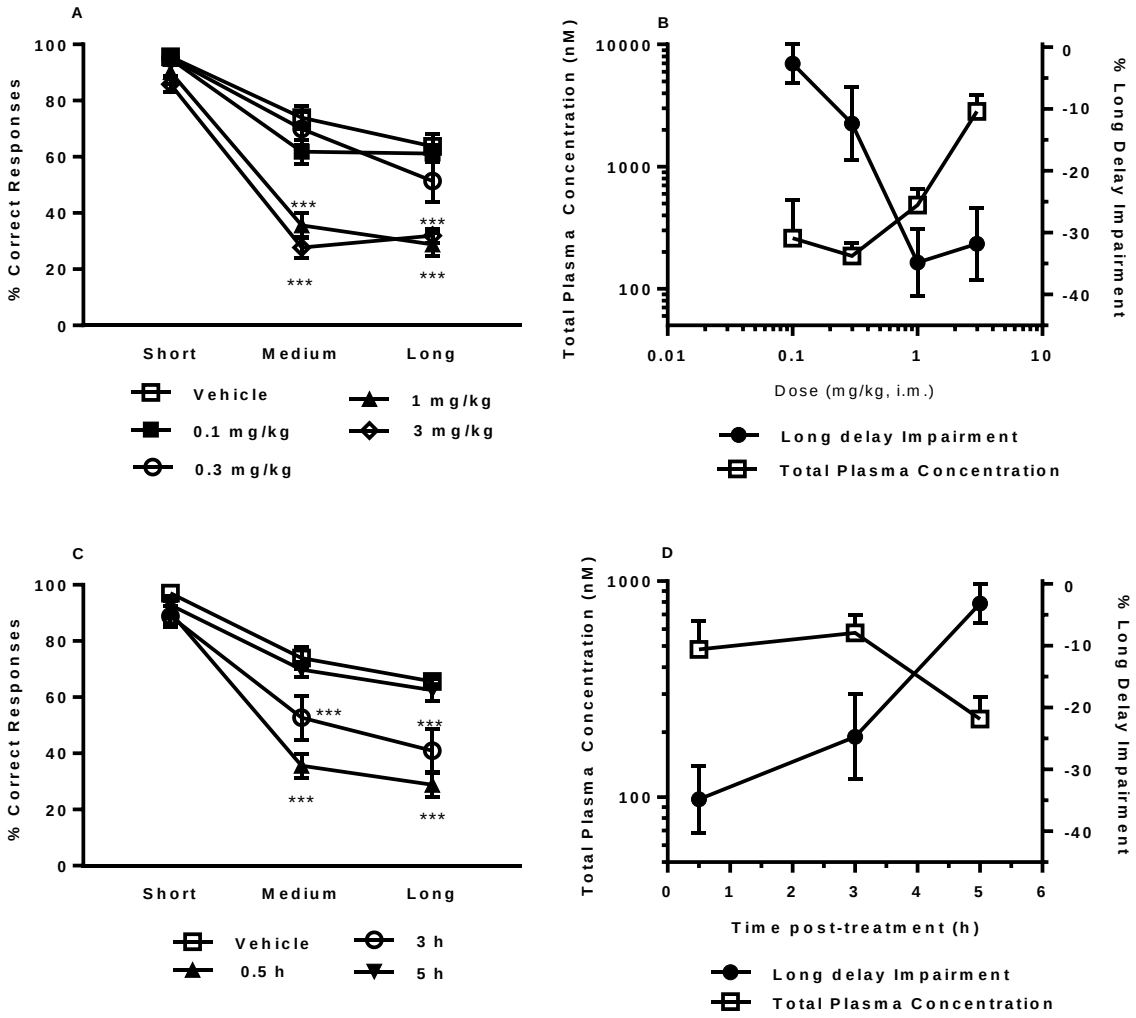

Figure 9

JPET Fast Forward. Published on September 27, 2017 as DOI: 10.1124/jpet.117.242784
This article has not been copyedited and formatted. The final version may differ from this version.

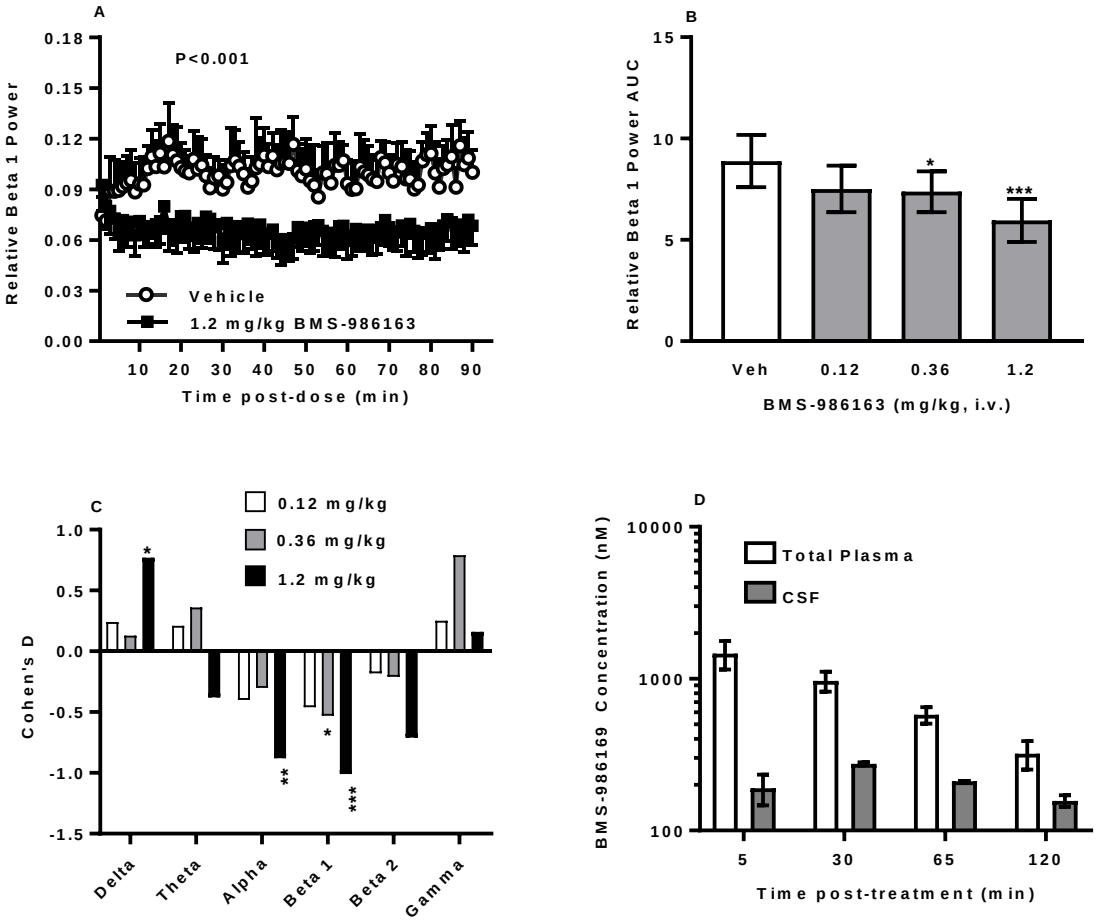

Figure 10

Supplemental Information

Bristow LJ et al: Preclinical Characterization of (*R*)-3-((3*S*,4*S*)-3-fluoro-4-(4-hydroxyphenyl)piperidin-1-yl)-1-(4-methylbenzyl)pyrrolidin-2-one (BMS-986169), a Novel, Intravenous, Glutamate N-Methyl-D-Aspartate 2B (GluN2B) Receptor Negative Allosteric Modulator with Potential in Major Depressive Disorder.

Journal Pharmacology Experimental Therapeutics

Supplemental Table 1 Behavioral checklist used for observational studies in cynomolgus monkeys. Abnormal behavior was calculated as a composite of behavioral items 2 + 4 + 6 + 7 + 10 + 11. Hallucinatory/dissociative-like behavior was calculated as a composite of behavioral items 7 + 11.

Item	Description
1	Normal Gross Motor: Normal locomotion, walking, swinging
2	Abnormal Gross Motor (stereotypy): Repetitive gross motor including pacing, circling, somersaulting, repetitive motions that cannot be interrupted
3	Normal static: Normal monkey positions - sitting normally
4	Abnormal static: Awkward positions, freezing, huddling
5	Grooming: manipulation of skin or fur with hands (maybe feet) and mouth including scratching
6	Other abnormal: non stereotypy abnormal behavior, including motor incoordination, falling, tics, huddling and new behaviors
7	Hallucinatory-like: abnormal tracking, hyper-tracking, hyper-vigilance, excessive checking, tracking nothing, staring into space, parasitoic-like grooming, manipulation of the air, orienting to nothing
8	Normal investigation: looking around normally, fiddling with object and other materials in cage
9	Normal oral/facial: open mouth, yawning, grimace, eye brow raising and other facial movement
10	Abnormal oral/facial: droopy faced, open mouth
11	Dissociative-like behavior: vacant stare, glassy eyed
12	Physiological: nystagmus, drooling, vomiting, pupil dilation

Supplemental Table 2 Evaluation of BMS-986169 at other pharmacological targets.

Target	Species	Assay type	Result
Adenosine A2a receptor	Human	Binding	IC50 >30 μM
Adrenergic α1B receptor	Human	Binding	IC50 >30 μM
Adrenergic α1D receptor	Human	Binding	IC50 >30 μM
Adrenergic α2A receptor	Human	Binding	IC50 >30 μM
Adrenergic α2C receptor	Human	Binding	IC50 >30 μM
Adrenergic β1 receptor	Human	Binding	IC50 >30 μM
Adrenergic β2 receptor	Human	Binding	IC50 >30 μM
Cannabinoid CB1 receptor	Human	Binding	IC50 >30 μM
Dopamine D1 receptor	Human	Binding	IC50 >30 μM
Dopamine D2 receptor	Human	Binding	IC50 >30 μM
Histamine H1 receptor	Human	Binding	IC50 >30 μM
Histamine H2 receptor	Human	Binding	IC50 >30 μM
Muscarinic M2 receptor	Human	Binding	IC50 >30 μM
Opioid kappa receptor	Human	Binding	IC50 >30 μM
Opioid mu receptor	Human	Binding	IC50 >30 μM
Serotonin 5HT1B receptor	Human	Binding	IC50 >30 μM
Serotonin 5HT2A receptor	Human	Functional; agonist	EC50 >10 μM
Serotonin 5HT2B receptor	Human	Functional; agonist	EC50 >10 μM
Serotonin 5HT4 receptor	Human	Binding	IC50 >30 μM
Dopamine transporter	Human	Binding	IC50 >30 μM
Norepinephrine transporter	Human	Binding	IC50 >30 μM
Serotonin transporter	Human	Binding	IC50 >30 μM
Androgen receptor	Rat	Binding	IC50 >150 μM
Estrogen alpha receptor	Human	Binding	IC50 >150 μM
Glucocorticoid receptor	Human	Binding	IC50 = 61 μM
Progesterone receptor	Human	Binding	IC50 ~75 μM
Calcium Channel L type (Cav1.2)	Human	Functional; antagonist	IC50 = 14.5 μM
Calcium Channel T type (Cav3.2)	Human	Functional; activator	EC50 >25 μM
Cardiac Sodium Channel (NAV1.5)	Human	Functional; antagonist	IC50 = 19 μM
GABA-A (α1β2γ2) receptor	Rat	Functional; antagonist	IC50 >30 μM
GABA-A (α1β2γ2) receptor	Rat	Functional; potentiator	EC50 >30 μM
GABA-A (α5β2γ2) receptor	Rat	Functional; antagonist	IC50 >30 μM
Nicotinic Acetylcholine α1 receptor	Rat	Functional; antagonist	IC50 = 28.8 μM
Nicotinic Acetylcholine α4β2 receptor	Rat	Functional; agonist	EC50 >30 μM
Nicotinic Acetylcholine α7 receptor	Rat	Functional; antagonist	IC50 >30 μM
NMDA GluN1a/GluN2A receptor	Human	Functional; agonist	EC50 >30 μM
NMDA GluN1a/GluN2A receptor	Human	Functional; antagonist	IC50 >30 μM
NMDA GluN1a/GluN2B receptor	Human	Functional; agonist	EC50 >30 μM
Acetylcholinesterase	Human	Enzyme inhibition	IC50 >30 μM
Monoamine oxidase A	Human	Enzyme inhibition	IC50 >30 μM
Monoamine oxidase B	Human	Enzyme inhibition	IC50 >30 μM
Phosphodiesterase 3	Human	Enzyme inhibition	IC50 >50 μM
Phosphodiesterase 4	Human	Enzyme inhibition	IC50 >50 μM

Supplemental Table 3 BMS-986169 concentrations in plasma, brain tissue and CSF achieving 50% GluN2B occupancy (Occ50) after i.v. dosing in rats or mice.

Compound/ Species/ Study Type	**Total Plasma Occ50 Concentration (95% CL)**	**Brain Tissue Occ50 Concentration (95% CL)**	**CSF Occ50 Concentration (95% CL)**
BMS-986169/ Rat/ Occupancy Dose Response	199 nM (147 - 263)	571 (335 - 935)	Not Determined
BMS-986169/ Rat/ Occupancy Time Course	73 nM (64 - 84)	319 nM (249 - 400)	3.5 nM (2.5 - 4.6)
BMS-986163/ Rat/ Occupancy Dose Response	157 nM (130 - 189)	348 nM (240 - 502)	Not Determined
BMS-986163/ Rat/ Occupancy Dose Response & Time Course; satellite groups tested in parallel with in vivo [^{3}H]MK-801 binding studies	210 nM (170 - 258)	662 nM (506 - 862)	Not Determined
BMS-986169/ Mouse/ FST	102 nM (61 - 160)	404 nM (255 - 617)	Not Determined

Supplemental Table 4 Plasma and brain BMS-986169 concentrations and GluN2B occupancy in experimental or satellite animals (n = 4/group) dosed in parallel with mice tested in the FST, NSF and LMA assays.

Model	Agent Dosed/ Subjects	Time min	Dose mg/kg	Total Plasma BMS-986169 mean ± S.D. (nM)	Brain Tissue BMS-986169 mean ± S.D. (nM)	% GluN2B Occupancy mean ± S.E.M.
FST	BMS-986169/ Experimental	~ 25	0.3	91 ± 37	288 ± 115	41.9 ± 3.4
			0.56	94 ± 52	318 ± 183	65.5 ± 7.2
			1	268 ± 128	749 ± 215	73.3 ± 2.3
			3	760 ± 332	1640 ± 586	92.3 ± 3.7
NSF	BMS-986163/ Satellites	15	1	336 ± 27	626 ± 114	86 ± 4
			3	965 ± 84	4823 ± 420	101 ± 0.4
			10	2905 ± 296	5422 ± 1530	101 ± 0.4
LMA	BMS-986169/ Satellites	15	3	1561 ± 270	3438 ± 442	96.4 ± 1.2
			10	4854 ± 1476	11830 ± 1510	97.4 ± 1.4
			30	21407 ± 2550	29107 ± 4924	99.7 ± 0.5

Supplemental Table 5 Effect of BMS-986169 treatment on rat hippocampal fEPSP amplitude and slope following application of high frequency stimulation (HFS) to induce LTP. Results are the mean ± S.E.M. % increase over baseline during the last 5 min of the recording period after HFS application and were analyzed by one tailed, paired t test, *P<0.05.

Treatment	Time post dose	fEPSP Amplitude (mean ± S.E.M.)			
		Baseline	HFS-1	HFS-2	HFS-3
Vehicle (n = 5)	24 h	99.2 ± 0.6	157.3 ± 5.2	166.6 ± 6.3	170.2 ± 6.1
BMS-986169 1 mg/kg (n = 5)	24 h	101.2 ± 1.0	162.2 ± 1.3	176.6 ± 2.9	180.1 ± 4.3
Vehicle (n = 7)	24 h	100.9 ± 0.6	147.6 ± 7.0	160.8 ± 11.5	162.5 ± 13.9
BMS-986169 3 mg/kg (n = 7)	24 h	104.3 ± 2.3	173.7 ± 5.5 *	192.6 ± 9.5 *	199.3 ± 9.0 *
Vehicle (n = 8)	72 h	102.1 ± 0.8	157.5 ± 2.7	168.3 ± 2.5	169.5 ± 3.7
BMS-986169 3 mg/kg (n = 8)	72 h	101.5 ± 0.2	159.4 ± 6.8	176.5 ± 9.0	180.8 ± 9.9

Treatment	Time	fEPSP Slope (mean ± S.E.M.)			
		Baseline	HFS-1	HFS-2	HFS-3
Vehicle (n = 5)	24 h	99.1 ± 0.7	185 ± 7.3	208.4 ± 8.3	217.8 ± 8.2
BMS-986169 1 mg/kg (n = 5)	24 h	101.6 ± 1.0	200.3 ± 2.2 *	225.4 ± 6.4 *	233.9 ± 8.0 *
Vehicle (n = 7)	24 h	100.9 ± 0.8	171.7 ± 11.0	197.8 ± 16.7	205.1 ± 19.5
BMS-986169 3 mg/kg (n = 7)	24 h	104.1 ± 1.6	217.3 ± 13.5 *	268 ± 29.7 *	285 7 ± 32.3 *
Vehicle (n = 8)	72 h	102.3 ± 0.7	181 ± 7.5	204.7 ± 8.0	209.5 ± 6.4
BMS-986169 3 mg/kg (n = 8)	72 h	101.4 ± 0.3	192.2 ± 10.0	222.2 ± 13.0	235.5 ± 14.8

Supplemental Table 6 Total plasma BMS-986169 concentrations determined on completion of testing in cynomolgus monkeys dosed with BMS-986169.

Study	Time Post-Dose	Dose mg/kg, i.m.	Total Plasma BMS-986169 Mean ± S.D. (nM)
Behavioral Observation (n = 4/dose)	~ 75 min	1	620 ± 90
		3	1883 ± 310
		5.6	4460 ± 686
		10	10260 ± 5362
List-Delayed Match to Sample (n = 7-9/dose)	~ 1 h	0.1	260 ± 271
	~ 1 h	0.3	185 ± 52
	~ 1 h	1	483 ± 174
	~ 1 h	3	2827 ± 1058
	~ 3.5 h	1	576 ± 117
	~ 5.5 h	1	230 ± 62

Supplemental Table 7 Summary of statistical results for qEEG time course data in cynomolgus monkeys treated with BMS-986163 (i.v.; n = 6). For each subject relative power (i.e. power in a band/absolute power) was determined as the average value in 1 min time bins across the 90 min recording period. Results were analyzed by 2 way ANOVA with time and treatment as repeated factors followed by Holm-Sidak post-hoc comparisons comparing treatment to vehicle. Significant results are shown in bold type; *P<0.05, **P<0.01, ***P<0.001 compared to vehicle.

Power Band	**2 way Repeated Measures ANOVA Results**	**Holm-Sidak Post-hoc Test comparing treatment vs Vehicle**
Delta (0.5-4 Hz)	Time: F(89,445)=0.969; P=0.5613 **Treatment: F(3,15)=3.511; P=0.0416** Interaction: F(267,1335)=0.8863; P=0.8914	0.12 mg/kg P=0.7488 0.36 mg/kg P=0.9467 **1.2 mg/kg P=0.0242***
Theta (4-9 Hz)	Time: F(89,445)=1.029; P=0.4161 Treatment: F(3,15)=0.9806; P=0.4281 Interaction: F(267,1335)=1.116; P=0.1171	0.12 mg/kg P=0.7993 0.36 mg/kg P=0.7993 1.2 mg/kg P=0.7993
Alpha (9-13Hz)	Time: F(89,445)=0.8397; P=0.8426 **Treatment: F(3,15)=4.704; P=0.0165** Interaction: F(267,1335)=1.136; P=0.0833	0.12 mg/kg P=0.3384 0.36 mg/kg P=0.3384 **1.2 mg/kg P=0.0071****
Beta 1 (13-19 Hz)	Time: F(89,445)=0.827; P=0.8631 **Treatment: F(3,15)=10.07; P=0.0007** **Interaction: F(267,1335)=1.389; P=0.0002**	**0.12 mg/kg P=0.0258*** **0.36 mg/kg P=0.0258*** **1.2 mg/kg P=0.0002*****
Beta 2 (20-30 Hz)	Time: F(89,445)=0.8089; P=0.8893 Treatment: F(3,15)=2.33; P=0.1157 Interaction: F(267,1335)=1.12; P=0.1085	0.12 mg/kg P=0.7414 0.36 mg/kg P=0.7414 1.2 mg/kg P=0.0708
Gamma (30-55 Hz)	Time: F(89,445)=0.8816; P=0.7639 Treatment: F(3,15)=1.525; P=0.2488 Interaction: F(267,1335)=0.9142; P=0.8201	0.12 mg/kg P=0.6435 0.36 mg/kg P=0.1645 1.2 mg/kg P=0.6435

Supplemental Table 8 Summary of statistical results for qEEG AUC data in cynomolgus monkeys treated with BMS-986163 (i.v.; n = 6). For each subject the area under the relative power curve for each power band was calculated from the time course data and analyzed by ANOVA with treatment as the repeated factor followed by Dunnett's post-hoc test. Significant results are shown in bold type; *P<0.05, **P<0.01, ***P<0.001 compared to vehicle.

Power Band	**One way Repeated Measures ANOVA Treatment Effect**	**Dunnett's Post-Hoc Test Comparing Treatment vs Vehicle**
Delta (0.5-4 Hz)	**F(3,15)=3.541; P=0.0405**	0.12 mg/kg P=0.7446 0.36 mg/kg P=0.9413 **1.2 mg/kg P=0.0233***
Theta (4-9 Hz)	F(3,15)=0.9874; P=0.4252	0.12 mg/kg P=0.9505 0.36 mg/kg P=0.7521 1.2 mg/kg P=0.7531
Alpha (9-13Hz)	**F(3,15)=4.742; P=0.0161**	0.12 mg/kg P=0.3902 0.36 mg/kg P=0.5603 **1.2 mg/kg P=0.0061****
Beta 1 (13-19 Hz)	**F(3,15)=10.07; P=0.0007**	0.12 mg/kg P=0.0529 **0.36 mg/kg P=0.032*** **1.2 mg/kg P=0.0002*****
Beta 2 (20-30 Hz)	F(3,15)=2.349; P=0.1136	0.12 mg/kg P=0.8616 0.36 mg/kg P=0.8109 1.2 mg/kg P=0.059
Gamma (30-55 Hz)	F(3,15)=1.518; P=0.2507	0.12 mg/kg P=0.7287 0.36 mg/kg P=0.1403 1.2 mg/kg P=0.9225

Supplemental Figure 1 Inhibition of [^{3}H]Ro 25-6981 binding to membranes prepared from rat forebrain. Results show the mean ± S.E.M. % inhibition of binding determined from 3-4 independent studies.

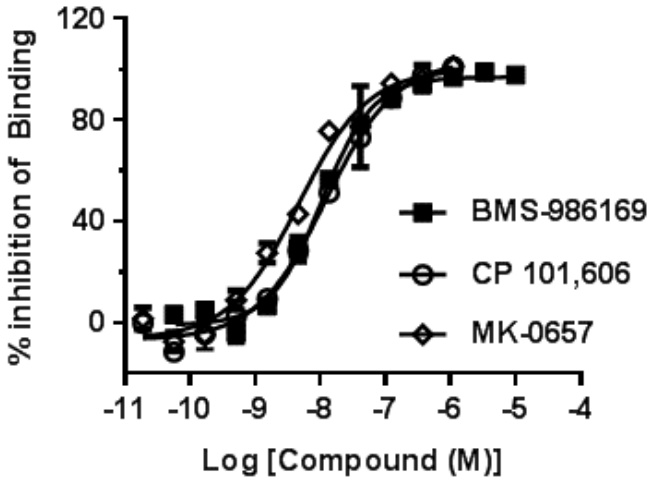

Supplemental Figure 2 Representative inhibition curves for displacement of [^{3}H]Ro 25-6981 binding to membranes prepared from A) human frontal cortex or B) cynomolgus monkey frontal cortex. Results show the mean ± S.E.M. % inhibition of binding (n = 2 replicates) determined in an individual experiment.

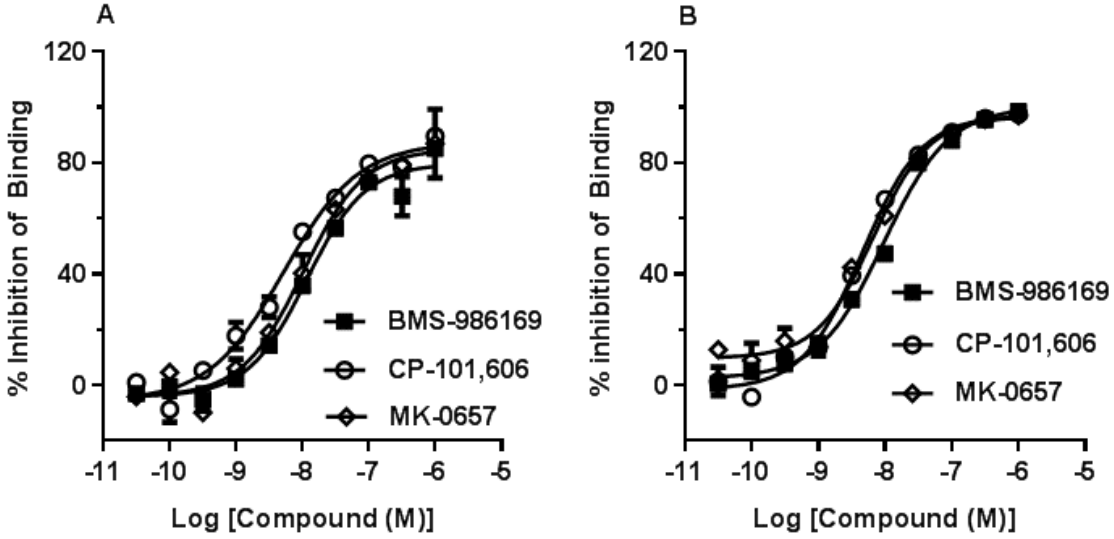

Supplemental Figure 3 A) Relationship between brain tissue BMS-986169 concentration and ex vivo GluN2B occupancy determined 15 min after i.v. administration of BMS-986169 or BMS-986163 in individual rats. B) Time course of exposure in plasma and CSF after i.v. administration of 3 mg/kg BMS-986169 in rats. Results are presented as the mean ± S.D. BMS-986169 concentration (plasma n = 4/group; CSF n = 3-4/group). Rat plasma protein binding = 7.8% free. C) Measured versus predicted GluN2B occupancy for same subjects as shown in panel B. Predicted occupancy was calculated using the CSF BMS-986169 concentration and the rat *in vitro* binding Ki value.

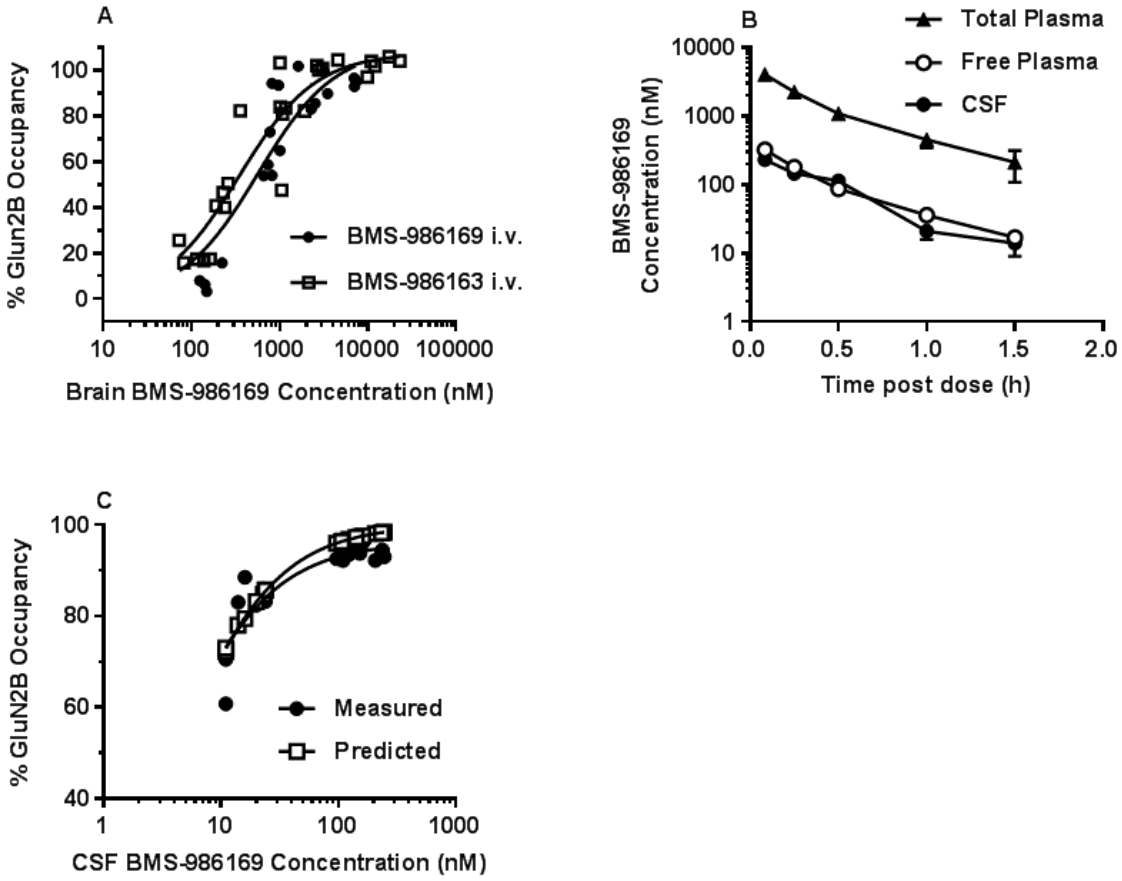

Supplemental Figure 4 Relationship between A) total plasma and B) brain tissue BMS-986169 concentration and ex vivo GluN2B occupancy in rats dosed with the phosphate prodrug BMS-986163 via previously implanted jugular vein catheters. Subjects were from satellite groups run in parallel with animals receiving [^{3}H]MK-801 and plots show combined results from both the dose response (i.e. 0.1 - 10 mg/kg; 15 min pretreatment) and time course (3 mg/kg; 15 -120 min) studies.

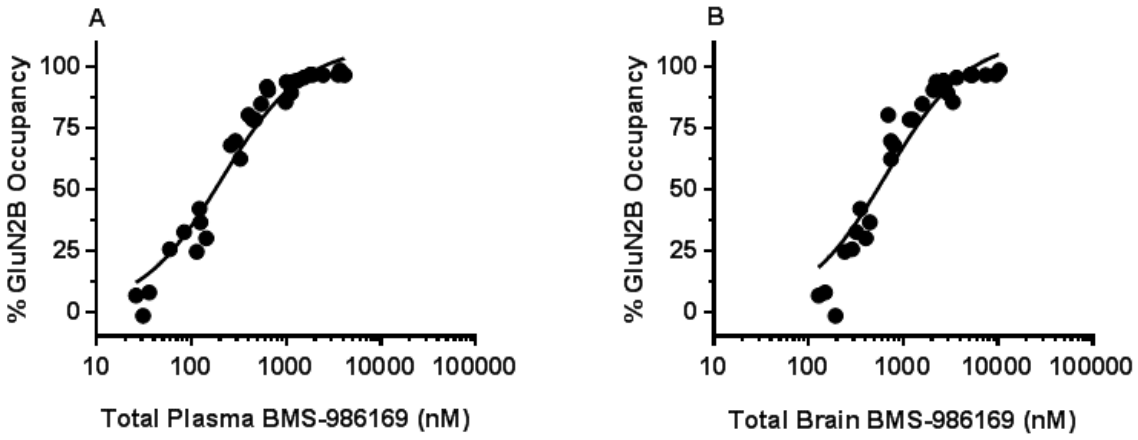

Supplemental Figure 5 A) Relationship between GluN2B receptor occupancy and total plasma or brain tissue BMS-986169 concentration for individual mice tested in the FST assay. Plasma and brain tissue were collected immediately after completion of behavioral assessment i.e. ~25 min after i.v. dosing with BMS-986169. B) GluN2B occupancy/dose relationship in FST mice or satellite mice dosed in parallel with NSF or LMA subjects (n = 4/group). Results are presented as the mean ± S.E.M. % occupancy determined 15 min (NSF, LMA) or ~25 min (FST) after treatment with BMS-986169 (FST, LMA) or BMS-986163 (NSF).

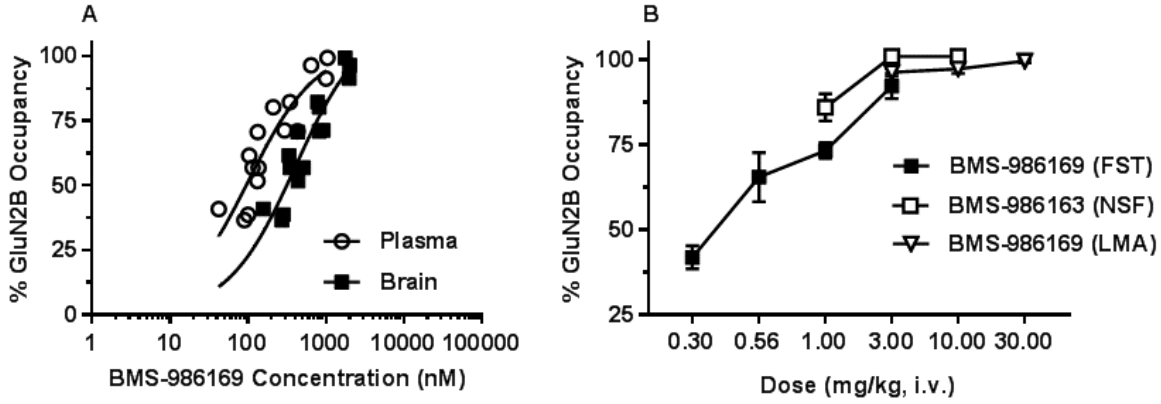

Supplemental Figure 6 Effect of ketamine in the NSF assay determined 24 h after i.p. dosing in mice. Results show the mean ± S.E.M. A) latency to feed in the novel environment and B) quantity (mg) of food consumed in the home cage during a 30 min period beginning immediately after testing in the novel environment (n = 12-15/group). Results were analyzed by ANOVA followed by Dunnett's t test, * P<0.05 compared to vehicle (Veh).

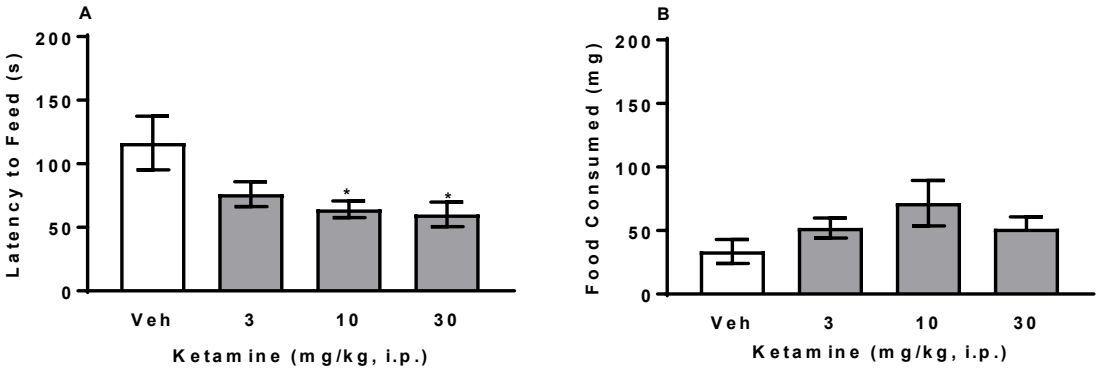

Supplemental Figure 7 Effect of ketamine (i.m.) on spontaneous behavior in cynomolgus monkeys (n = 12). Results are presented as the mean ± S.E.M. total score for A) all abnormal behaviors and B) dissociative/hallucinogenic-like behaviors observed in each time bin after treatment. Results were analyzed by 2 way RM ANOVA followed by Dunnett's post-hoc test; *** P<0.001, ** P<0.01 compared to saline treatment. ANOVA results were as follows: A) abnormal behaviors: treatment effect: $F(3,33) = 5.871$, $P = 0.0025$; time effect: $F(4,44) = 8.327$, $P < 0.0001$; interaction: $F(12,132) = 1.574$, $P = 0.1065$; B) dissociative/hallucinogenic behaviors: treatment effect: $F(3,33) = 4.892$, $P = 0.0064$; time effect: $F(4,44) = 15.02$, $P < 0.0001$; interaction: $F(12,132) = 2.102$, $P = 0.0207$.

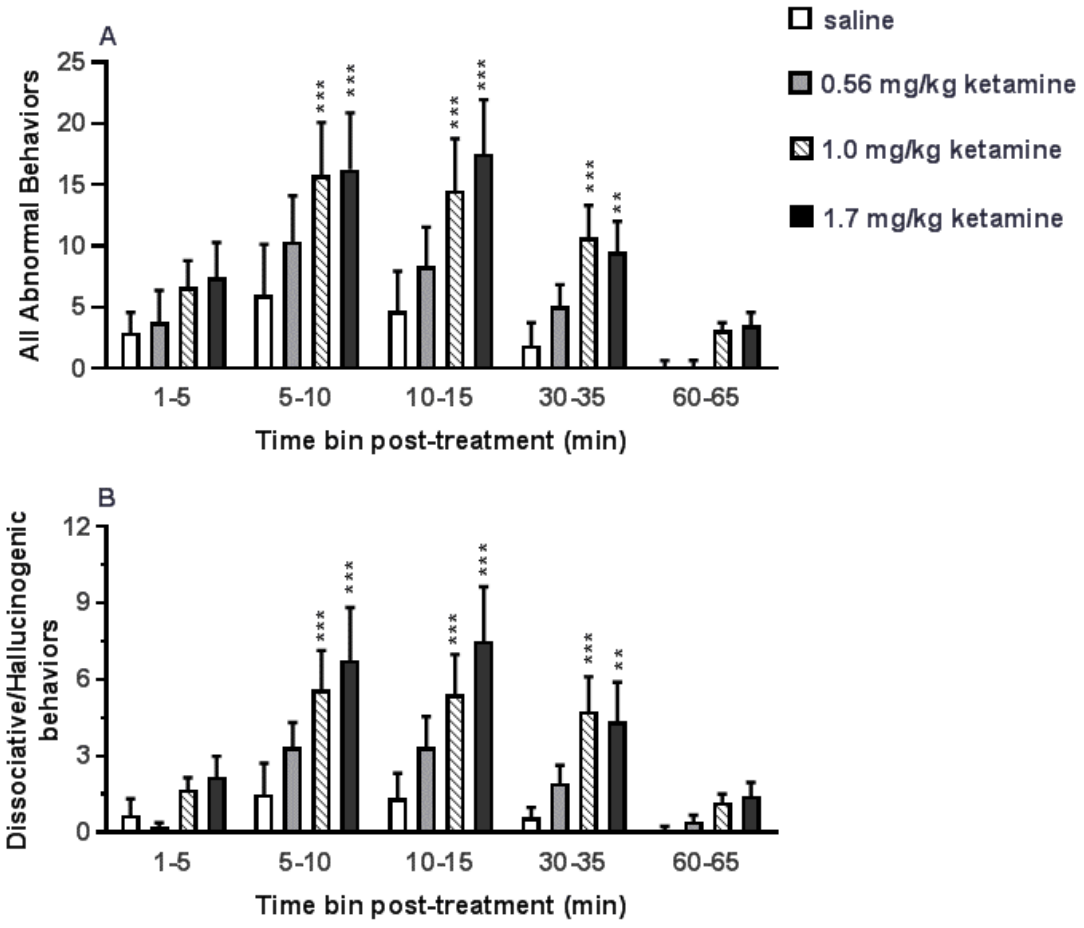

Supplemental Figure 8 Effect of BMS-986169 (i.m.) on performance measures in cynomolgus monkeys performing the CANTAB list-DMS task (n = 9). Results are presented as the mean ± S.E.M. % task completed (A and C) or the mean ± S.E.M. latency to respond (B and D). Subjects for the dose response study (A and B) were tested 30 min after treatment; subjects for the time course study were dosed with 1 mg/kg BMS-986169. Results were analyzed by one way repeated measures ANOVA followed by Dunnett's post-hoc test; **P<0.01 compared to vehicle. ANOVA results for treatment effects were as follows: A) F(4,32) = 1.911, P = 0.1327; B) F(4,32) = 4.135, P = 0.0082; C) F(3,24) = 3.596, P = 0.0282; D) F(3,24) = 1.132, P=0.3562.

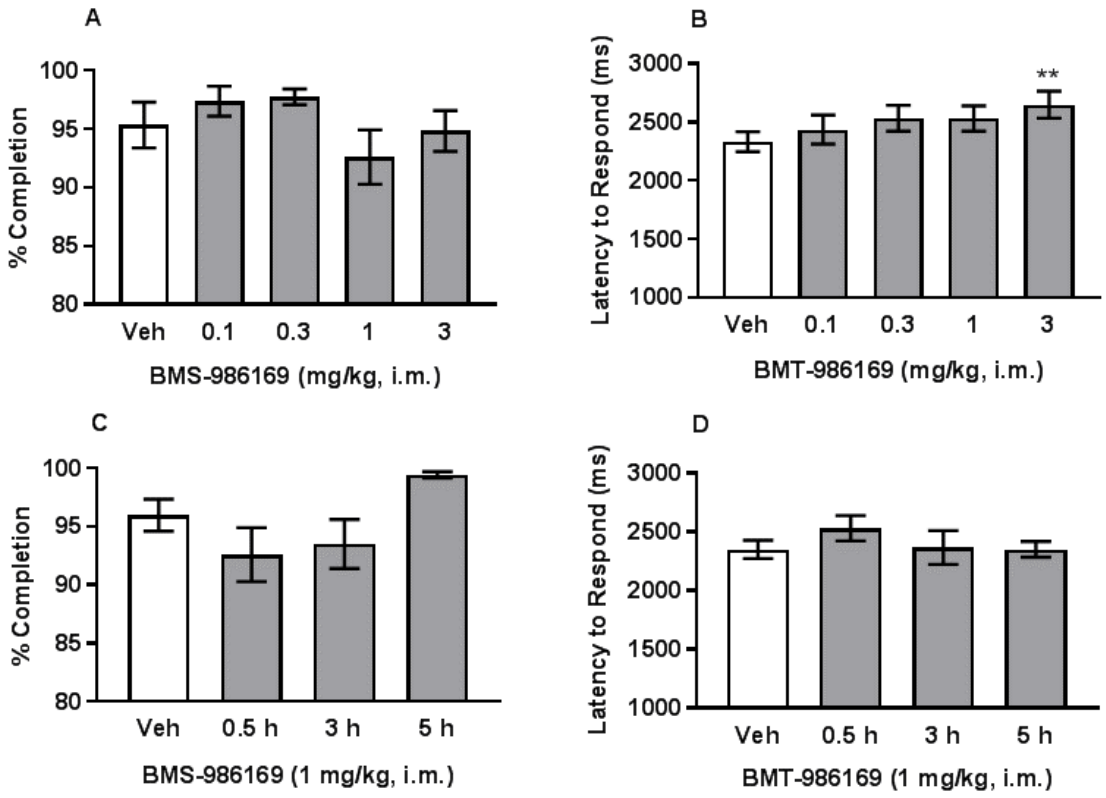

Supplemental Figure 9 A) Total plasma concentration time course and B) CSF concentration and predicted GluN2B occupancy determined 30 min after i.m. dosing with BMS-986169 in cynomolgus monkeys. Results are presented as the mean ± S.D. BMS-986169 concentration (n = 2/group).

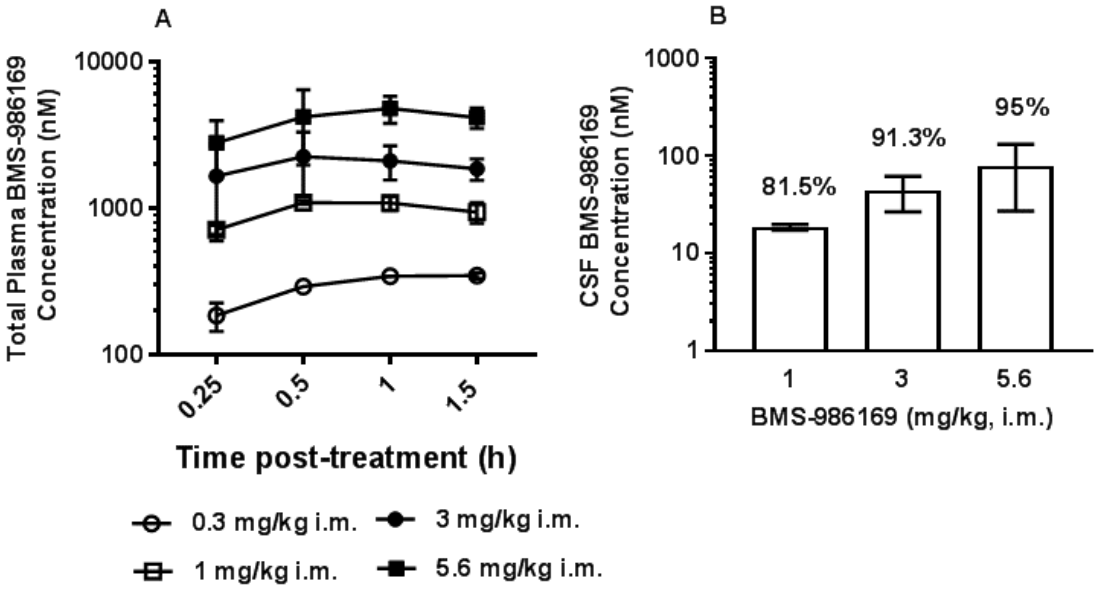

Supplemental Figure 10 Time course of the qEEG effects of i.v. administration of 0.12 mg/kg BMS-986163 on relative power in the A) delta band (0.5-4 Hz), B) theta band (4-9 Hz), C) alpha band (9-13 Hz), D) beta 1 band (13-19 Hz), E) beta 2 band (20-30 Hz) and F) gamma band (30-55 Hz) in cynomolgus monkeys. Results are presented as the mean ± S.E.M. (n = 6) relative power determined at 1 min intervals after dosing. Statistical results are summarized in Supplemental Table 7.

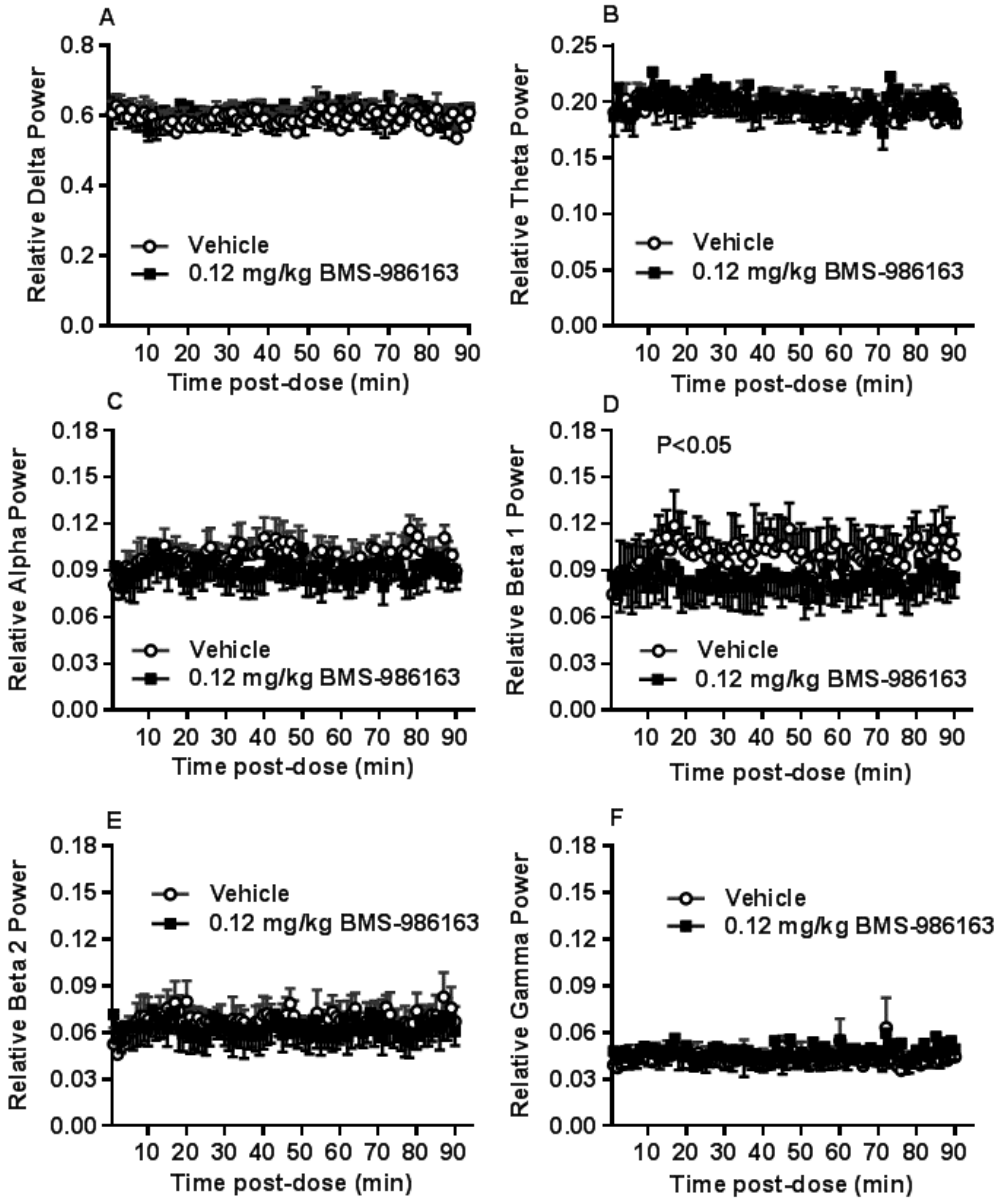

Supplemental Figure 11 Time course of the qEEG effects of i.v. administration of 0.36 mg/kg BMS-986163 on relative power in the A) delta band (0.5-4 Hz), B) theta band (4-9 Hz), C) alpha band (9-13 Hz), D) beta 1 band (13-19 Hz), E) beta 2 band (20-30 Hz) and F) gamma band (30-55 Hz) in cynomolgus monkeys. Results are presented as the mean ± S.E.M. (n = 6) relative power determined at 1 min intervals after dosing. Statistical results are summarized in Supplemental Table 7.

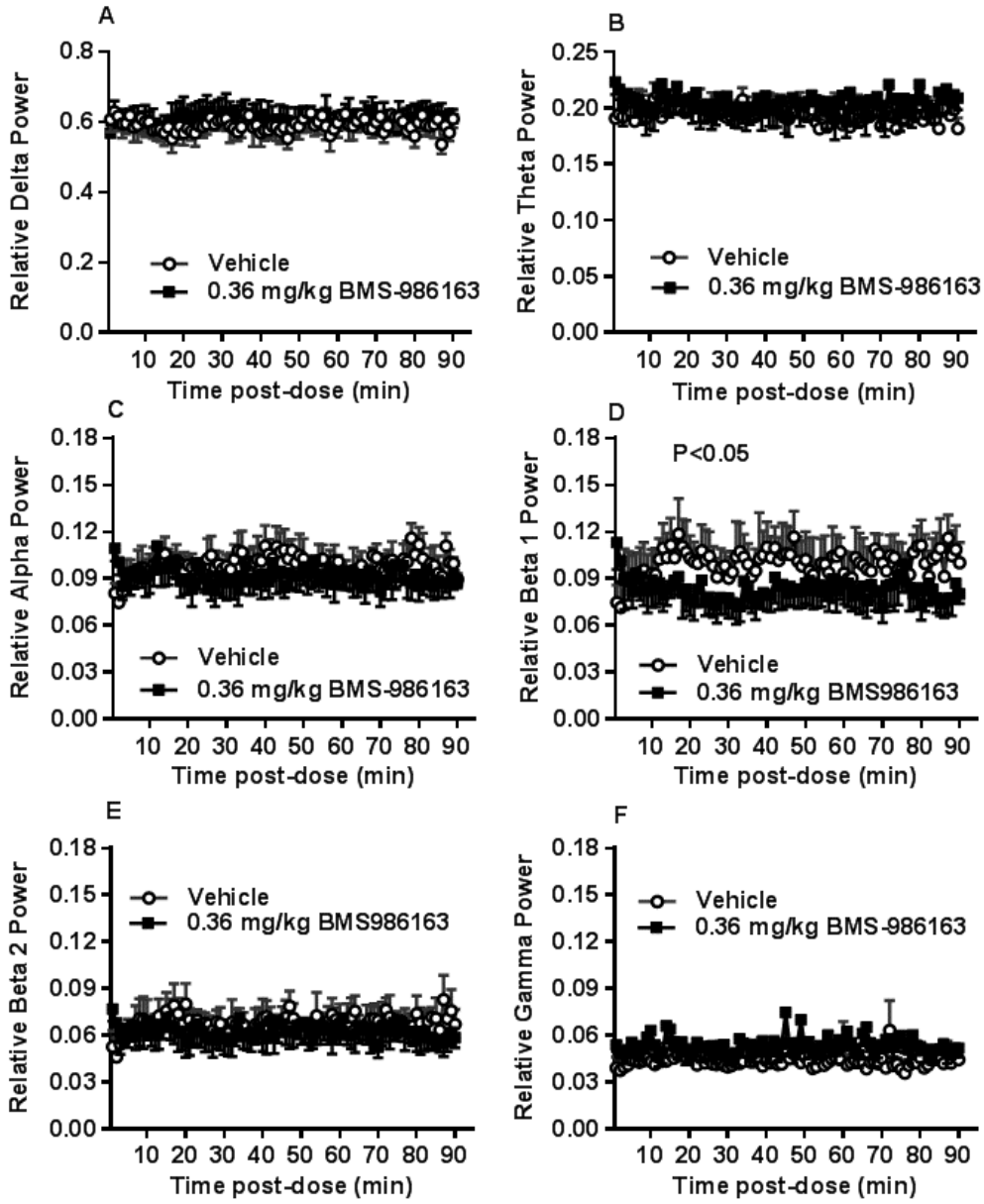

Supplemental Figure 12 Time course of the qEEG effects of i.v. administration of 1.2 mg/kg BMS-986163 on relative power in the A) delta band (0.5-4 Hz), B) theta band (4-9 Hz), C) alpha band (9-13 Hz), D) beta 1 band (13-19 Hz), E) beta 2 band (20-30 Hz) and F) gamma band (30-55 Hz) in cynomolgus monkeys. Results are presented as the mean ± S.E.M. (n = 6) relative power determined at 1 min intervals after dosing. Statistical results are summarized in Supplemental Table 7.

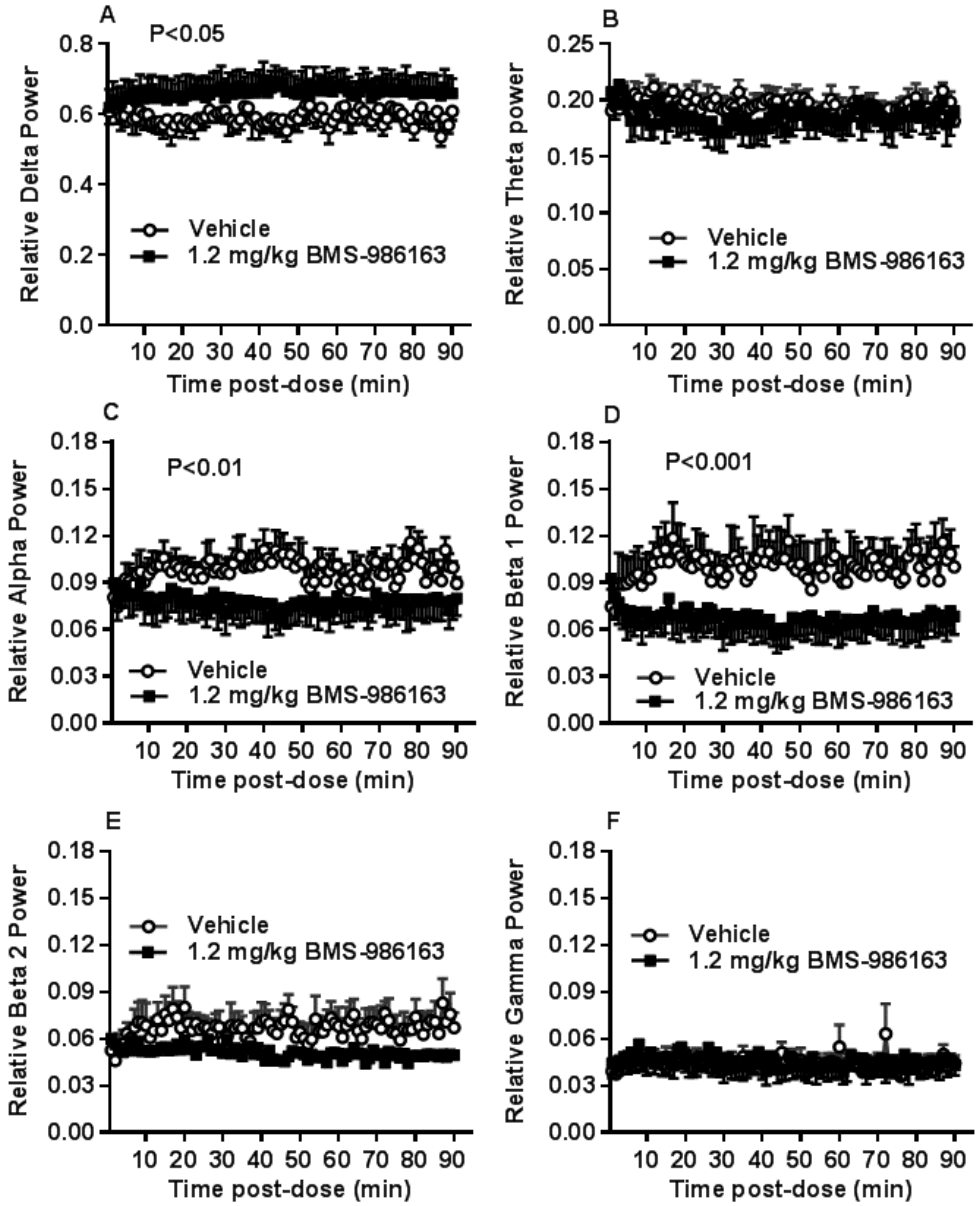

Supplemental Figure 13 Effect of i.v. administration of BMS-986163 on the qEEG relative power AUC in the A) delta band (0.5-4 Hz), B) theta band (4-9 Hz), C) alpha band (9-13 Hz), D) beta 1 band (13-19 Hz), E) beta 2 band (20-30 Hz) and F) gamma band (30-55 Hz) in cynomolgus monkeys. Results are presented as the mean ± S.E.M. AUC (n = 6) and were analyzed by repeated measures ANOVA followed by Dunnett's post-hoc test; *P<0.05, **P<0.01, ***P<0.001. Individual ANOVA results are reported in Supplemental Table 8.